

Dynamics of Information Spreading in Online Social Networks

Sai Zhang, Ke Xu, *Member, IEEE*, Xi Chen, *Student Member, IEEE*, and Xue Liu, *Member, IEEE*

Abstract—Online social networks (OSNs) are changing the way information spreads throughout the Internet. A deep understanding of information spreading in OSNs leads to both social and commercial benefits. In this paper, dynamics of information spreading (e.g., how fast and widely the information spreads against time) in OSNs are characterized, and a general and accurate model based on Interactive Markov Chains (IMCs) and mean-field theory is established. This model shows tight relations between network topology and information spreading in OSNs, e.g., the information spreading ability is positively related to the heterogeneity of degree distributions whereas negatively related to the degree-degree correlations in general. Further, the model is extended to feature the time-varying user behavior and the ever-changing information popularity. By leveraging the mean-field theory, the model is able to characterize the complicated information spreading process (e.g., the dynamic patterns of information spreading) with six parameters. Extensive evaluations based on Renren's data set illustrate the accuracy of the model, e.g., it can characterize dynamic patterns of video sharing in Renren precisely and predict future spreading dynamics successfully.

Index Terms—online social networks, complex networks, information spreading, network topology, dynamic patterns.

I. INTRODUCTION

WITH the fast development of the Internet and Web2.0, online social networks (OSNs) generated by the Web applications are playing an important role in information spreading throughout the Internet. Getting, publishing and sharing information with forums, video-sharing sites (VSSes) and social networking sites (SNSes) are becoming increasingly popular. A recent report¹ shows that as of May 2013, almost 72% online U.S. adults use SNSes, up from 67% in late 2012 and only 8% in February 2005. In August 2013², there were about 500 million tweets per day on Twitter and a peak of 143,199 tweets per second was observed during the airing

of *Castle in the Sky*³. SNSes can influence user's purchase decisions. Statistics⁴ show that 74% consumers make their purchase decisions based on SNSes. In emergency situations such as fires and earthquakes, information spreading in SNSes can also provide valuable knowledge that is crucial in life-saving. Approximately 96% earthquakes of Japan Meteorological Agency (JMA) seismic intensity scale 3 or more are detected merely by monitoring tweets [1]. Moreover, SNSes even facilitate the mobilization of mass movements⁵. Therefore, it is important and necessary to study the nature of information spreading in OSNs to promote viral marketing, improve social benefits, and maintain social security in practical aspects, as well as understand the characteristics of complex networks and individual behaviors in scientific aspects.

Numerous works [2–5] have studied various spreading processes in networks. Due to the complexity of underlying network topology and the diversity of collective behaviors, these models focus on simplified scenarios where several important factors of information spreading are missing. Previous works on epidemic spreading [6–13] and rumor diffusion [14–17] have constructed rigorous theories to describe spreading processes in different circumstances. These works use tools of mean-field and dynamical systems to derive precise results in characterizing spreading dynamics. Since the processes and mechanisms of epidemic and rumor spreading are quite different from those of information spreading in OSNs, we should establish new theoretical models to characterize information spreading in OSNs. In this paper, we first elaborate a general mechanism of information spreading in realistic OSNs and establish a probabilistic model in the framework of *Interacting Markov Chains* (IMCs) [18]. Then based on the mean-field principle, we transform the probabilistic model into a deterministic version characterized by a non-linear dynamical system. By analyzing this system, we show that information spreading in OSNs is mainly characterized by the following three arguments: spreading *threshold*, *prevalence* and *efficiency*. Our work reveals how the defined model parameters and network topology influence these arguments.

The process of information spreading relies on both the spreading mechanism and the underlying network topology. On one hand, several existing models [4, 5] are limited by the fact that they ignore the network topology and only characterize the spreading process in global perspectives. On

Sai Zhang is with the Institute for Interdisciplinary Information Sciences, Tsinghua University, Beijing, 100084, China (e-mail: zs11235@gmail.com). Ke Xu is with the Department of Computer Science & Technology, Tsinghua University, Beijing, 100084, China (e-mail: xuke@mail.tsinghua.edu.cn). Xi Chen and Xue Liu are with the School of Computer Science and the Department of Electrical and Computer Engineering, McGill University, Montreal, QC H3A 0E9, Canada (e-mail: {xchen100,xueliu}@cs.mcgill.ca).

This work was supported in part by the 973 Programs (2011CBA00300, 2011CBA00301, 2012CB315803), the 863 Program (2013AA013302), the NSFC Projects (61033001, 61170292, 61361136003), the New Generation Broadband Wireless Mobile Communication Network of the National Science and Technology Major Projects (2012ZX03005001), and the EU MARIE CURIE ACTIONS EVANS (PIRSES-GA-2010-269323).

¹Pew Research Center's Internet & American Life Project. <http://www.pewinternet.org/2013/08/05/methods-15/>.

²New Tweets per second record, and how!. <https://blog.twitter.com/2013/new-tweets-per-second-record-and-how>.

³Castle in the Sky. http://en.wikipedia.org/wiki/Castle_in_the_Sky.

⁴Social Networks Influence 74% Consumers Buying Decisions. <http://sproutsocial.com/insights/social-networks-influence-buying-decisions/>.

⁵Technology and Globalization. <http://www.globalization101.org/uploads/File/Technology/tech2012.pdf>.

the other hand, other approaches [2, 3] modeling information spreading based on the network structure cannot work when the network is implicit or even unknown. In this paper, a more accurate model is established by considering two key quantities of network topology, i.e., degree distributions (the first-order correlation) and degree-degree correlations (the second-order correlation), which balances the global-local paradox. We derive analytic relations between network heterogeneity and information spreading, and demonstrate that the positive degree-degree correlations inhibit information spreading in general. This theoretical result has been confirmed by previous experiments.

Previous studies [19–22] have shown that the dynamics of online media exhibit great burstiness, diurnal patterns and periodicity. However, existing “static” models of epidemic and rumor spreading cannot fully characterize these features. To fill this gap, we propose another spreading model with time-varying parameters, which describes user behavior and information popularity in time domain. We further study how the temporal dynamics of model parameters affect the spreading process. Through analytic deductions, we find that the temporal dynamics of model parameters largely determine how information spreading evolves in OSNs. This facilitates us to learn realistic patterns with six reasonable parameters. To our knowledge, this is the first spreading model which characterizes the dynamic patterns of information spreading in realistic complex networks in closed forms. By testing on a data set of video sharing in Renren⁶, one of the largest SNSes in China, we show that our time-varying model can depict the spreading dynamics precisely. Furthermore, we verify that the time-varying model can successfully predict long-ranged dynamic patterns of information spreading given history data.

The rest of the paper is structured as follows. Section II describes our probabilistic model and gives the deterministic dynamical system derived by the model. Section III sums up the terminologies and notations used in the following sections and defines the spreading threshold, prevalence and efficiency. In Section IV, based on defined arguments we comprehensively study the impact of underlying network topology on information spreading in both uncorrelated and correlated heterogeneous networks. The spreading model with time-varying parameters and its analysis are given in Section V. Section VI carries out several numerical studies to verify previous analytic conclusions, and uses the Levenberg-Marquardt (LM) algorithm [23] to learn the dynamic patterns of video sharing in Renren based on the time-varying model. We also use the improved model to predict future dynamics of video sharing. Finally, we summarize related work in Section VII, conclude this paper and discuss our future work in Section VIII.

II. MODEL DESCRIPTION

Consider an undirected network $N = (V, E)$, where V denotes the set of vertices and $|V| = n$, and E denotes the set of edges. Note that we sometimes refer to vertices as users in OSNs. The information \mathcal{I} (e.g., a message, photo or video) spreads along its edges. We first divide the states of vertices

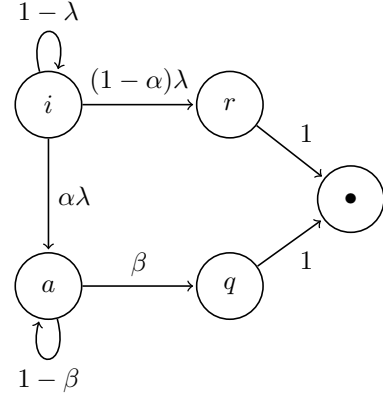


Fig. 1. State transition diagram. i , a , r , q are short for *ignorant*, *active*, *indifferent* and *quiet*, respectively.

into three kinds: *ignorant*, *active* and *indifferent*. Ignorant vertices are those who are unaware of \mathcal{I} , active vertices are those who are aware of \mathcal{I} and actually spread (e.g., forwarding or sharing in SNSes) it, and indifferent vertices are those who are aware of it but do not spread it. Since active vertices have spread \mathcal{I} , their ignorant neighbors can be activated with a certain probability. Based on the fact that active vertices can only affect their neighbors in a limited time duration due to the popularity decay, we assume that active vertices become *quiet* (a new state in which they get no influence on their neighbors any more) with a certain probability spontaneously.

Figure 1 illustrates our model. In network N , there are four kinds of vertices, *ignorant*, *active*, *indifferent* and *quiet*. Information \mathcal{I} spreads in N based on the following mechanisms:

- (1) While keeping their states unchanged with probability $1 - \lambda$, ignorant vertices with active neighbors can be aware of \mathcal{I} to become active and indifferent with probability λ .
- (2) Vertices who are aware of \mathcal{I} and are as yet inactive will become active with probability α or be indifferent with probability $1 - \alpha$.
- (3) Active vertices become quiet spontaneously with probability β .

From the above rules, we find that indifference and quietness are two final states of vertices. In other words, the process of information spreading is also the process of vertex state decay with indifference and quietness as its final states. Thus we can add another state “•” to uniformly describe all vertices knowing \mathcal{I} . Since indifferent and quiet vertices both belong to this kind of vertices and cannot affect their neighbors, they become “•” absolutely (see Fig. 1). Note that the process of information spreading or vertex state decay terminates when there is no active vertices in the network.

We have shown that each vertex in N changes its state according to Fig. 1 and its neighbor’s states. This process is what IMCs [18] deal with. Therefore, keeping the above spreading mechanisms in mind, we get⁷ the following set of coupled differential equations (non-linear dynamical system) that describe the dynamics of information spreading on a

⁶Renren. <http://www.renren.com/>

⁷Derivation details are given in Appendix A.

mean-field level [16].

$$\frac{di_k(t)}{dt} = -\lambda k i_k(t) \sum_{k'} P(k' | k) a_{k'}(t), \quad (1a)$$

$$\frac{da_k(t)}{dt} = \alpha \lambda k i_k(t) \sum_{k'} P(k' | k) a_{k'}(t) - \beta a_k(t), \quad (1b)$$

$$\frac{dr_k(t)}{dt} = (1 - \alpha) \lambda k i_k(t) \sum_{k'} P(k' | k) a_{k'}(t), \quad (1c)$$

$$\frac{dq_k(t)}{dt} = \beta a_k(t), \quad (1d)$$

where $i_k(t)$, $a_k(t)$, $r_k(t)$, $q_k(t)$ denote the fractions of vertices with degree k in the states of ignorant, active, indifferent and quiet at time t , respectively, and integer k' ranges from 0 to k_c , which is the largest degree⁸ in network N . Obviously, we have $i_k(t) + a_k(t) + r_k(t) + q_k(t) = 1$. Note that we will clarify more definitions, e.g., vertex degree, degree distribution and $P(k' | k)$, in the next section. If we denote $i(t)$, $a(t)$, $r(t)$, $q(t)$ as the vertex fractions of four states, we also have $i(t) + a(t) + r(t) + q(t) = 1$. In addition, we assume that at $t = 0$, the initial conditions of the system are $i(0) = (n-1)/n \approx 1$, $a(0) = 1/n \approx 0$, $r(0) = 0$ and $q(0) = 0$, where “ \approx ” makes sense if n is large enough.

Note that the defined network N is a kind of *undirected Markovian random network* [6], whose topology is completely determined by the degree distribution $P(k)$ and the conditional probability $P(k' | k)$. In other words, we assume in approximation that all higher-order correlation functions can be obtained as random combinations of $P(k)$ and $P(k' | k)$.

III. TERMINOLOGIES, NOTATIONS AND NEW DEFINITIONS

In this section, we list some common terminologies and notations in network science, which are frequently used in this paper. We also give the exact definitions of three important arguments that characterize the dynamics of information spreading in networks.

A. Relevant Terminologies and Notations

The *degree* [24] of a vertex in an undirected network is defined as the the number of edges attached to it. We denote the largest degree in a network as k_c and always use lower-case k to denote degrees. The *degree distribution* $P(k)$ [24] describes the fraction of vertices with degree k . We denote the average degree as $\langle k \rangle$, which equals to $\sum_k k P(k)$. Similarly, the average square degree $\langle k^2 \rangle$ equals to $\sum_k k^2 P(k)$. Note that we always approximate the summation of sequence by its integral to simplify computations.

Degree distribution characterizes the network topology from a local perspective, and different networks with the same degree distribution share similar topologies. In this paper, we consider the scale-free (SF) networks, the most common networks in real world [24]. The degree distribution of an

SF network follows a power law. Formally speaking, in SF networks, the degree distribution $P(k)$ is defined as [24]

$$P(k) = \begin{cases} Z k^{-\gamma} & \text{if } k \geq m, \\ 0 & \text{otherwise,} \end{cases} \quad (2)$$

where m is the minimum degree of the network and is set to 1 in this paper, and the normalization constant Z approximately equals to $(\gamma-1)m^{\gamma-1}$. In order to ensure finite average degrees in SF networks, we shall keep $\gamma > 2$. Particularly, the case of $\gamma = 3$ is the degree distribution of networks generated by the Barabási-Albert (BA) model [25].

A network is *heterogeneous* [13] if there are vertices whose degrees are significantly larger than the average degree. Otherwise, the network is *homogeneous* [13]. We can use $\langle k^2 \rangle / \langle k \rangle$ to quantify the network heterogeneity approximately, i.e., a network usually becomes more heterogeneous if its $\langle k^2 \rangle / \langle k \rangle$ gets larger. Thus, heterogeneity characterizes the irregularity of network topology from the degree distribution perspective. It is not hard to find that in an SF network, as the exponent γ gets smaller, the network is more heterogeneous (large degree appears with higher probability).

Most realistic networks [24] exhibit non-trivial connectivity patterns. For instance, most OSNs [26–28] present *assortativity*, while the Web networks and the Internet [29] are always *disassortative*. These connectivity trends among vertices with different degrees cannot be characterized by degree distributions. Actually, various connectivity patterns influence the network topology drastically and result in different degree distributions.

Degree distribution is often called the *first-order correlation* [10] in complex networks. Generally speaking, we define the conditional probabilities $P(k', k'', \dots, k^{(n)} | k)$, the probabilities of vertices with degree k attaching simultaneously to other n vertices with corresponding degrees $k', k'', \dots, k^{(n)}$, to characterize higher-order (the *n*th-order) correlations. The network is referred as *uncorrelated* [10] if there are no conditional probabilities in the network connectivity. Otherwise, the network is *correlated* [10]. It is known that in Markovian networks [6], which is the main concern in the following sections, only the degree distribution $P(k)$ and the degree-degree correlations $P(k' | k)$ are taken into account. If we define the joint probability distribution $P(k, k')$ [24] as the probability of randomly selecting an edge that connects a vertex with degree k and another vertex with degree k' , and define the *excess degree distribution* $q(k) \triangleq \sum_{k'} P(k, k')$ [24] that equals to $k P(k) / \langle k \rangle$, we have

$$P(k, k') = q(k) P(k' | k). \quad (3)$$

Therefore, the joint distribution $P(k, k')$ totally determines the topology of the Markovian network. In addition, we have $P(k, k') = q(k) q(k')$ in uncorrelated networks, and this leads to $P(k' | k) = q(k')$. These results are frequently used in the following sections.

Another measure that characterizes the second-order correlations is the *average nearest neighbors degree* (ANND) $\langle k_{nn} \rangle \triangleq \sum_{k'} k' P(k' | k)$ [30], i.e., the average neighbors degree of vertices with degree k . In uncorrelated networks, we have $\langle k_{nn} \rangle = \langle k^2 \rangle / \langle k \rangle$ independent on k .

⁸For brevity, we make k_c approach infinity in certain cases. We will see this approximation is reasonable as well as computationally helpful in the following sections.

B. Three Arguments Characterizing Information Spreading

As $t \rightarrow \infty$, the process of information spreading reaches its equilibrium when there is no active vertices in the network. What matters most is the condition under which the information \mathcal{I} spreads out, and the range and the velocity of the spreading process. We now define three arguments that describe these aspects.

Definition 1: The spreading prevalence \mathcal{P} is defined as $r_\infty + q_\infty$, where $r_\infty \triangleq \lim_{t \rightarrow \infty} r(t)$ and $q_\infty \triangleq \lim_{t \rightarrow \infty} q(t)$.

The spreading prevalence \mathcal{P} characterizes the final spreading range, i.e., the fraction of vertices aware of the information when the spreading process ends. It is obvious that $0 < \mathcal{P} \leq 1$.

Consider the model parameter function $\rho(\alpha, \beta, \gamma) = \alpha\gamma/\beta$, which is denoted as ρ for short. In fact, ρ reflects the ability and potential of information spreading. Concretely, if vertices in network N get and spread the information \mathcal{I} easily (correspond to large λ and large α , respectively), and at the same time, \mathcal{I} loses its popularity slowly (corresponds to small β), then \mathcal{I} will spread in a wide range. Otherwise, \mathcal{I} will be trapped in a narrow area.

Definition 2: If there is a real number $\rho_c \geq 0$ satisfying $\mathcal{P} > 0$ when $\rho > \rho_c$, we refer ρ_c as the spreading threshold.

If a function $f(t)$ evolves with a dominant term $e^{t/\tau}$, it is clear that the growth time scale τ determines the evolution velocity of f , i.e., the smaller τ is, the faster f evolves. In order to describe the velocity of the spreading process, we define the spreading efficiency as follows.

Definition 3: The spreading efficiency \mathcal{E} is defined as the reciprocal of the growth time scale τ in information spreading, i.e., $\mathcal{E} \triangleq 1/\tau$.

Note that in Definition 3 we treat the information spreading process as the evolution of $a(t)$. We will clarify this definition with the help of some analytic results derived in Section IV.

IV. INFORMATION SPREADING CHARACTERISTICS

In this section, we study the characteristics of information spreading in uncorrelated and correlated heterogeneous networks, based on the arguments defined in Section III. We focus on how the model parameters and the network topology, i.e., the degree distributions and the degree-degree correlations, influence the information spreading process. The philosophy here is to study naive networks first, add higher-order correlations gradually, and investigate how the correlations influence the spreading process.

A. Uncorrelated Heterogeneous Networks

We begin our study with the uncorrelated heterogeneous networks, where we concern how the degree distributions affect the spreading dynamics. To clarify this, we focus on SF networks and analyze exponent γ 's function on spreading. We have the following theorems to characterize the dynamics of information spreading.

Theorem 1: In uncorrelated heterogeneous networks, the spreading threshold ρ_c equals to $\langle k \rangle / \langle k^2 \rangle$. In other words, the prevalence $\mathcal{P} > 0$ if and only if $\rho > \langle k \rangle / \langle k^2 \rangle$. In particular,

in SF networks, we have

$$\rho_c = \begin{cases} \frac{\gamma-3}{\gamma-2} & \text{if } \gamma > 3, \\ 0 & \text{if } 2 < \gamma \leq 3. \end{cases} \quad (4)$$

Proof: See Appendix B. ■

Remark 1: We have shown that $\langle k^2 \rangle / \langle k \rangle$ can be regarded as the measure of network heterogeneity. Hence the threshold in uncorrelated heterogeneous networks is negatively related to the network heterogeneity. In other words, the more heterogeneous the uncorrelated network is, the more easily the information spreads out. According to Theorem 1, when $2 < \gamma \leq 3$, SF networks are heterogeneous enough to make the spreading threshold disappear.

Given the explicit expression of degree distribution of SF networks, we can get the following theorem that characterizes the spreading range.

Theorem 2: In uncorrelated SF networks, the spreading prevalence \mathcal{P} has the following expressions in different cases.

(1) $2 < \gamma < 3$:

$$\mathcal{P} \sim \rho^{1/(3-\gamma)}, \quad (5)$$

(2) $3 < \gamma < 4$:

$$\mathcal{P} \sim \left(1 - \frac{\rho_c}{\rho}\right)^{1/(\gamma-3)}, \quad (6)$$

(3) $\gamma > 4$ and $\gamma \notin \mathbb{N}$:

$$\mathcal{P} \sim 1 - \frac{\rho_c}{\rho}, \quad (7)$$

where “ \sim ” means “be approximately proportional to”. When $\gamma \in \mathbb{N}$, the expression of \mathcal{P} should be analyzed case by case. Particularly, in the case of $\gamma = 3$, we have

$$\mathcal{P} \sim e^{-1/\rho}. \quad (8)$$

Proof: See Appendix C. ■

Remark 2: We find from Theorem 2 that the spreading prevalence in SF networks is determined by both the model parameters (i.e., ρ) and the network topology (i.e., the exponent γ). For example, in heterogeneous networks where $2 < \gamma < 3$, the heterogeneity increases the spreading prevalence if $\rho < 1$, while decreases it otherwise. Therefore, the network topology, e.g., heterogeneity, influences the spreading process in complicated manners. We will discuss more details in Section IV-B.

Theorem 1 and Theorem 2 are about the stable state of the spreading process, whereas the following theorem describes the temporal behavior of information spreading.

Theorem 3: In uncorrelated heterogeneous networks, the growth time scale τ of information spreading is negatively related to the network heterogeneity, i.e., $\langle k^2 \rangle / \langle k \rangle$, which is the reciprocal of threshold ρ_c . More precisely, we have

$$\tau = \frac{1/\beta}{\rho/\rho_c - 1}. \quad (9)$$

Particularly, in SF networks, the efficiency \mathcal{E} has the expression

$$\mathcal{E} = \begin{cases} \frac{\alpha\lambda(\gamma-2) - \beta(\gamma-3)}{\gamma-3} & \text{if } \gamma > 3, \\ \infty & \text{if } 2 < \gamma \leq 3. \end{cases} \quad (10)$$

Proof: See Appendix D. ■

Remark 3: It is shown in Theorem 3 that an increasing heterogeneity improves the efficiency of information spreading, i.e., it improves the spreading speed. For instance, the infinite efficiency contributes to almost instantaneous rise of spreading incidence in more heterogeneous SF networks where $2 < \gamma \leq 3$.

B. Correlated Heterogeneous Networks

Previous empirical studies [26–28] have found that OSNs exhibit assortativity, i.e., vertices with large degrees tend to connect to vertices with large degrees, while vertices with small degrees prefer to connect to vertices with small degrees. This phenomenon is not well explained by researchers, and it is conjectured for several reasons, e.g., preferential attachment [25] and proximity bias [31]. No matter what makes the assortativity in OSNs, it has a significant impact on the edge creation, network evolution and network topology. Thus it is necessary to study how these (positive) second-order correlations affect the dynamics of information spreading. We conduct our analysis of Markovian networks equipped with first-order and second-order correlations in this subsection.

We know that $i_k(t) = 1 - a_k(t) - r_k(t) - q_k(t)$. By omitting⁹ terms of $\mathcal{O}(a^2)$, Eq. 1b can be written as

$$\frac{da_k(t)}{dt} \approx \sum_{k'} L_{kk'} a_{k'}(t), \quad (11)$$

or

$$\frac{d\mathbf{a}}{dt} = \mathbf{L}\mathbf{a}, \quad (12)$$

where the Jacobian matrix $\mathbf{L} = \{L_{kk'}\}$ is defined as

$$L_{kk'} = -\beta\delta_{kk'} + \alpha\lambda k P(k' | k), \quad (13)$$

and $\delta_{kk'}$ is the Kronecker delta symbol. The solutions of Eq. 12 imply that the behavior of $a_k(t)$ is given by the linear combination of exponential functions with the form $e^{\lambda_i t}$, where λ_i is the eigenvalue of \mathbf{L} .

By linear stability analysis [10] of the system (12), we conclude the following theorem that determines the spreading threshold of Markovian networks.

Theorem 4: The connectivity matrix $\mathbf{C} = \{C_{kk'}\}$ is defined as $C_{kk'} = kP(k' | k)$. The spreading threshold of the Markovian networks is

$$\rho_c = \frac{1}{\Lambda_m}, \quad (14)$$

where Λ_m is the largest eigenvalue of \mathbf{C} .

Proof: See Appendix E. ■

Remark 4: Comparing to Theorem 1, Theorem 4 states a more general result on spreading threshold in Markovian networks where the degree-degree correlations are considered. At the same time, Eq. 14 agrees with the result of Theorem 1 in unstructured networks with no second-order correlations, where \mathbf{C} has the unique eigenvalue $\Lambda_m = \langle k^2 \rangle / \langle k \rangle$.

⁹We cannot perform this approximation all the time as $a_k(t)^2$, $r_k(t)a_k(t)$ and $q_k(t)a_k(t)$ are not always small enough to be omitted during the spreading process. But this approximation works well in this part of analysis.

In order to study the influence of positive degree-degree correlations on the spreading process precisely, we here define the conditional probability $P(k' | k)$ satisfying [32]

$$P(k' | k) = (1 - \theta)q(k') + \theta\delta_{kk'}, \quad (15)$$

where $0 \leq \theta < 1$. Note that if $\theta = 0$, there is no degree-degree correlations in the network. As θ increases, the network owns higher positive correlations, i.e., stronger assortativity.

Before stating main results on the influence of degree-degree correlations on the spreading dynamics, we have the following corollary.

Corollary 1: The spreading threshold of correlated heterogeneous networks, where degree-degree correlations are defined as Eq. 15, is negatively related to degree-degree correlations, i.e.,

$$\rho_c \sim 1 / \left(\frac{\langle k^2 \rangle}{\langle k \rangle} (1 - \theta) \right). \quad (16)$$

Proof: The connection matrix \mathbf{C} of SF networks can be written as $\mathbf{C} = \{(1 - \theta)kq(k') + \theta k\delta_{kk'}\}$. Thus we have

$$\det(\mathbf{C} - \Lambda \mathbf{I}) = f(\Lambda) \cdot \prod_{k=2}^{k_c} (\theta k - \Lambda),$$

where

$$f(\Lambda) = (\theta - \Lambda) \left(1 + (1 - \theta) \sum_{k=1}^{k_c} \frac{kq(k)}{\theta k - \Lambda} \right).$$

With regard to $f(\Lambda)$, we find that for any θ and $k = 1, \dots, k_c$, there is null point Λ_k locating in $(\theta k, \theta k + \varepsilon_k)$, where θk is the pole of $f(\Lambda)$ and $\varepsilon_k > 0$. Denote $\Lambda_m \in (\theta k_c, \theta k_c + \varepsilon_{k_c})$ as the maximum null point of $f(\Lambda)$, hence it is the largest eigenvalue of \mathbf{C} . To approximate Λ_m , we have

$$1 + (1 - \theta) \sum_{k=1}^{k_c} \frac{kq(k)}{\theta k - \Lambda_m} = 0,$$

which further gives

$$\Lambda_m - (1 - \theta) \sum_{k=1}^{k_c} \frac{kq(k)}{1 - \frac{\theta k}{\Lambda_m}} \approx \Lambda_m - \frac{\langle k^2 \rangle}{\langle k \rangle} (1 - \theta) = 0.$$

This implies Eq. 16. ■

Remark 4a: Corollary 1 implies that higher positive degree-degree correlations increase spreading threshold. In other words, correlations inhibit information spreading to some extent. Note that when the network is uncorrelated (i.e., $\theta = 0$), we also get $\Lambda_m = \langle k^2 \rangle / \langle k \rangle$ in the proof of Corollary 1. Hence we can treat Eq. 16 as the generalized result of Theorem 1 in correlated networks.

Based on Eq. 15, the system of Eqs. 1a to 1d becomes

$$\begin{aligned} \frac{di_k(t)}{dt} = & -(1 - \theta)\lambda k i_k(t) \sum_{k'} q(k') a_{k'}(t) \\ & - \theta \lambda k i_k(t) a_k(t), \end{aligned} \quad (17a)$$

$$\begin{aligned} \frac{da_k(t)}{dt} = & (1 - \theta)\alpha \lambda k i_k(t) \sum_{k'} q(k') a_{k'}(t) \\ & + (\theta \alpha \lambda k i_k(t) - \beta) a_k(t), \end{aligned} \quad (17b)$$

$$\frac{dr_k(t)}{dt} = (1 - \theta)(1 - \alpha)\lambda k i_k(t) \sum_{k'} q(k') a_{k'}(t) + \theta(1 - \alpha)\lambda k i_k(t) a_k(t), \quad (17c)$$

$$\frac{dq_k(t)}{dt} = \beta a_k(t), \quad (17d)$$

In this case, the relations between the network topology and spreading prevalence are more complicated than those in uncorrelated networks. We have the following theorem.

Theorem 5: In correlated SF networks, the function of the degree-degree correlations (i.e., θ) on the spreading prevalence \mathcal{P} is affected by both the model parameters (i.e., ρ) and the exponent γ of degree distributions.

Proof: See Appendix F. ■

Remark 5: Several previous studies [11, 16] concluded incomplete results about the impact of degree-degree correlations on the epidemic and rumor spreading. In [16], Nekovee *et al.* experimentally found that these correlations' influence on the final fractions of vertices hearing a rumor depends much on the rate of rumor diffusion. Theorem 5 gives the theoretical explanation behind this phenomenon in the framework of our model. In fact, the influence of degree-degree correlations on information spreading varies a lot along with different information spreading potentials and network degree distributions. Note that we do not concern about the impact of the largest degree k_c or the network size here. However, k_c and the finite network size indeed affect the spreading process as well [8]. In Section VI, we will find numerically that large k_c and network heterogeneity can balance out the torsion of the degree-degree correlations' influence on spreading caused by model parameters.

We have shown that if \mathbf{L} has n distinct eigenvalues, the system $d\mathbf{a}/dt$ has $e^{\lambda_1 t} \mathbf{r}_1, \dots, e^{\lambda_n t} \mathbf{r}_n$ as its fundamental solutions, where \mathbf{r}_i is the eigenvector of \mathbf{L} with respect to the eigenvalue λ_i where $i = 1, \dots, n$. Thus, $\mathbf{a}(t)$ is determined mainly by the maximum eigenvalue λ_m , i.e.,

$$a_k(t) \sim e^{\lambda_m t}.$$

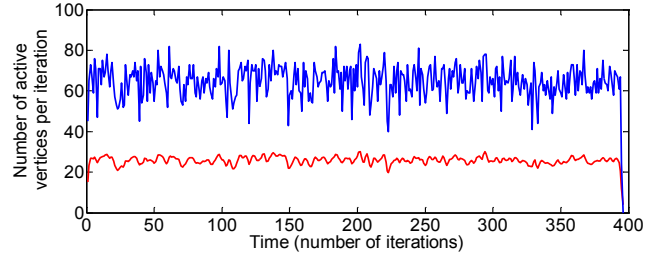
We have proven part of the following theorem.

Theorem 6: In correlated networks, the spreading efficiency \mathcal{E} is determined by the maximum eigenvalue of Jacobian matrix \mathbf{L} . In SF networks, we have

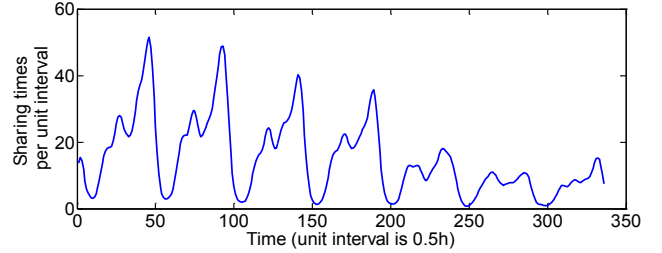
$$\mathcal{E} \sim \frac{\langle k^2 \rangle}{\langle k \rangle} (1 - \theta). \quad (18)$$

Proof: We have proved the first part of the theorem. For the remaining part, by the deduction similarly to that in Corollary 1, the maximum eigenvalue λ_m of \mathbf{L} equals approximately to $\alpha\lambda(1 - \theta)\langle k^2 \rangle / \langle k \rangle$. According to Definition 3, we get Eq. 18. ■

Remark 6: First, in uncorrelated networks, \mathbf{L} has the only eigenvalue $\alpha\lambda\langle k^2 \rangle / \langle k \rangle - \beta$, thus the conclusion of Theorem 6 agrees with Theorem 3. Second, the degree-degree correlations also inhibit the spreading process in the aspect of spreading efficiency. At the same time, the largest degree k_c that contributes to network heterogeneity also has great influence on the growth time scale of the spreading process. When $k_c \rightarrow \infty$, which usually results in the infinity of $\langle k^2 \rangle / \langle k \rangle$, the growth



(a) Simulated information spreading based on static model



(b) A video sharing in Renren

Fig. 2. Comparison of simulated and realistic spreading dynamics. (a) Time series (blue curve) of Monte Carlo simulated information spreading based on the model in Section II. To reduce rapid fluctuations in series, we apply the Gaussian smoothing (red curve). We generate the underlying SF network of 1,000 vertices according to the BA model. We set the model parameters as $\alpha = 0.5$, $\lambda = 0.5$ and $\beta = 0.5$. (b) Time series of a video sharing in Renren after the Gaussian smoothing.

time scale disappears. This implies an irresistible spreading in correlated heterogeneous networks. Actually, by bounding λ_m more precisely, we can get this conclusion without the restriction of specific degree-degree correlations. Given the Perron-Frobenius theorem, we have

$$\begin{aligned} \lambda_m^2 &\geq \min_k \frac{1}{k} \sum_{k'} k' \sum_l L_{kl} L_{lk'} \\ &= \min_k \sum_l \sum_{k'} \left(\alpha^2 \lambda^2 l P(l | k) k' P(k' | l) + \beta^2 \frac{k'}{k} \delta_{kl} \delta_{lk'} \right. \\ &\quad \left. - \alpha \lambda \beta \frac{l k'}{k} \delta_{kl} P(k' | l) - \alpha \lambda \beta k' \delta_{lk'} P(l | k) \right) \\ &= \min_k \left(\sum_l \left(\alpha^2 \lambda^2 l P(l | k) \langle l_{nn} \rangle (k_c) \right) - 2 \alpha \lambda \beta \langle k_{nn} \rangle (k_c) \right. \\ &\quad \left. + \beta^2 \right) \\ &\geq \min_k \beta^2 \left((\rho^2 \langle k_{nn} \rangle_{\min} - 2\rho) \langle k_{nn} \rangle (k_c) + 1 \right), \end{aligned}$$

where $\langle k_{nn} \rangle_{\min}$ denotes the minimum ANND in the network. Boguñá *et al.* [9, 10] have shown that the function $\langle k_{nn} \rangle (k_c)$ diverges as $k_c \rightarrow \infty$ in SF networks with $2 < \gamma \leq 3$. This leads to the divergence of λ_m and further the infinite \mathcal{E} .

V. IMPROVED MODEL WITH TIME-VARYING PARAMETERS

In previous sections, we assume that model parameters α , λ and β are invariant during the spreading process. This assumption is imprecise considering realistic circumstances and we can indeed take one step forward. In fact, there are only three kinds of vertex states in the information spreading process in OSNs, i.e., ignorant, active and indifferent. We

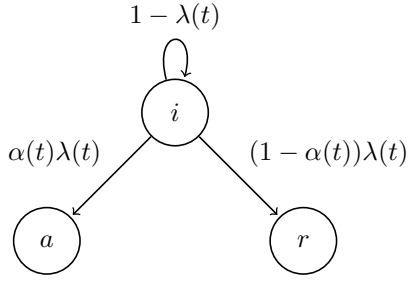


Fig. 3. State transition diagram of improved model. i , a , r are short for ignorant, active and indifferent, respectively.

add the quiet state derived from the active state to emphasize the nonpersistence of the impact of active vertices on their neighbors. It is unreasonable to assume that the probabilities of contacting and spreading the information are invariable from the beginning to the end. In realistic OSNs [21], probability λ that describes the likelihood of user being aware of the information is relevant to temporal patterns of user's online behaviors, e.g., λ varies over time in a day, or even over days of a week. Moreover, as probability α represents user's interest in the information, it is also changing depending on the fluctuation of information popularity.

Constant parameters fail to characterize temporal features in information spreading such as the dynamic patterns, i.e., the number change of new coming active vertices over time. Figure 2 illustrates the dynamic patterns of information spreading in an SF network based on our former static model and of a video sharing in Renren. From Fig. 2b, we find that in Renren the dynamics of information spreading own significant patterns, e.g., diurnal patterns, periodicity, sudden spikes and gradual decay, while the time series in Fig. 2a generated by our previous model seems to be random and has less notable tendencies. This distinct gap between the realistic example and the simulated result leads us to improve our model with time-varying parameters.

In this section, we first describe our new model with time-varying parameters, and then study the impact of varying parameters on information spreading.

A. Description of Improved Model

In our improved spreading model, where $\alpha \triangleq \alpha(t)$ and $\lambda \triangleq \lambda(t)$, we delete the state of quiet and the corresponding transition probability β . In this case, the information spreading process comes to an end along with the vanish of the information popularity, i.e., $\lim_{t \rightarrow \infty} \alpha(t) = 0$.

Figure 3 describes the process of vertex state decay. Note that as $\alpha(t) \rightarrow 0$, no vertex would spread the information and the process terminates. The system Eqs. 1a to 1d can be improved as

$$\frac{di_k(t)}{dt} = -\lambda(t)ki_k(t) \sum_{k'} P(k' | k) a_{k'}(t), \quad (19a)$$

$$\frac{da_k(t)}{dt} = \alpha(t)\lambda(t)ki_k(t) \sum_{k'} P(k' | k) a_{k'}(t), \quad (19b)$$

$$\frac{dr_k(t)}{dt} = (1 - \alpha(t))\lambda(t)ki_k(t) \sum_{k'} P(k' | k) a_{k'}(t), \quad (19c)$$

where $0 \leq \alpha(t) \leq 1$, $0 \leq \lambda(t) \leq 1$ and $\alpha_\infty = 0$.

B. Impacts of Time-Varying Parameters on Information Spreading

The active vertex is the key to the spreading process. Hence we focus on how time-varying parameters influence the change of the number of active vertices. The following theorem characterizes the spreading dynamics.

Theorem 7: In correlated heterogeneous networks, the changing rate of the number of active vertices is

$$\frac{d\mathbf{a}(t)}{dt} = \alpha(t)\lambda(t) \exp\left(\int_0^t \alpha(x)\lambda(x)dx\right) \mathbf{C}\mathbf{a}(0), \quad (20)$$

where $\mathbf{a}(0)$ is the initial fraction of active vertices in the network.

Proof: Similarly to Eq. 12, we can write Eq. 19b as

$$\frac{d\mathbf{a}(t)}{dt} = \mathbf{L}(t)\mathbf{a}(t), \quad (21)$$

where the Jacobian matrix $\mathbf{L}(t) = \{L_{kk'}(t)\}$ is defined by

$$L_{kk'}(t) = \alpha(t)\lambda(t)kP(k' | k).$$

Note that $\mathbf{L}(t) = \alpha(t)\lambda(t)\mathbf{C}$, where \mathbf{C} is the connectivity matrix defined in Theorem 4. Thus, $\mathbf{L}(t)$ is commutative, i.e., $\mathbf{L}(t_1)\mathbf{L}(t_2) = \mathbf{L}(t_2)\mathbf{L}(t_1)$ for all $t_1, t_2 \in (0, \infty)$. Define

$$\hat{\mathbf{L}}(t) \triangleq \int_0^t \mathbf{L}(x)dx,$$

and we have $\hat{\mathbf{L}}(t_1)\mathbf{L}(t_2) = \mathbf{L}(t_2)\hat{\mathbf{L}}(t_1)$. Based on these facts, we can easily get

$$\frac{d\hat{\mathbf{L}}^n(t)}{dt} = n\hat{\mathbf{L}}'(t)\hat{\mathbf{L}}^{n-1}(t).$$

We claim that $\mathbf{a}(t) = \exp \hat{\mathbf{L}}(t) \cdot \mathbf{a}(0)$ is the solution of Eq. 21. To prove this, take the derivative of $\mathbf{a}(t)$, we have

$$\begin{aligned} \frac{d\mathbf{a}(t)}{dt} &= \frac{d}{dt} \left(\sum_{n=0}^{\infty} \frac{\hat{\mathbf{L}}^n(t)}{n!} \cdot \mathbf{a}(0) \right) = \sum_{n=0}^{\infty} \hat{\mathbf{L}}'(t) \frac{\hat{\mathbf{L}}^n(t)}{n!} \cdot \mathbf{a}(0) \\ &= \hat{\mathbf{L}}'(t) \exp \hat{\mathbf{L}}(t) \cdot \mathbf{a}(0) = \mathbf{L}(t)\mathbf{a}(t), \end{aligned}$$

which is exactly Eq. 21.

Since \mathbf{C} is a real symmetric matrix, it can be diagonalized by orthogonal matrix. Furthermore, \mathbf{C} is nonsingular according to the proof of Corollary 1. Thus it is similar to the identity matrix, i.e., there exists orthogonal matrix \mathbf{P} such that $\mathbf{P}^{-1}\mathbf{C}\mathbf{P} = \mathbf{I}$. Therefore, we can rewrite the solution of Eq. 21 as

$$\begin{aligned} \mathbf{a}(t) &= \exp \hat{\mathbf{L}}(t) \cdot \mathbf{a}(0) = \exp \left(\int_0^t \mathbf{L}(x)dx \right) \mathbf{a}(0) \\ &= \exp \left(\int_0^t \alpha(x)\lambda(x)dx \cdot \mathbf{C} \right) \mathbf{a}(0) \\ &= \exp \left(\int_0^t \alpha(x)\lambda(x)dx \cdot \mathbf{P}\mathbf{I}\mathbf{P}^{-1} \right) \mathbf{a}(0) \end{aligned}$$

$$\begin{aligned}
&= \sum_{n=0}^{\infty} \frac{1}{n!} \left(\mathbf{P} \left(\int_0^t \alpha(x) \lambda(x) dx \cdot \mathbf{I} \right) \mathbf{P}^{-1} \right)^n \mathbf{a}(0) \\
&= \mathbf{P} \exp \left(\int_0^t \alpha(x) \lambda(x) dx \cdot \mathbf{I} \right) \mathbf{P}^{-1} \mathbf{a}(0) \\
&= \exp \left(\int_0^t \alpha(x) \lambda(x) dx \right) \mathbf{P} \mathbf{I} \mathbf{P}^{-1} \mathbf{a}(0) \\
&= \exp \left(\int_0^t \alpha(x) \lambda(x) dx \right) \mathbf{a}(0). \tag{22}
\end{aligned}$$

Therefore, together with Eq. 21, we finally get Eq. 20. ■

Remark 7: We here concern about the changing rate of the number of active vertices, i.e., $da(t)/dt$, where $a(t) = \sum_k P(k) a_k(t)$. According to Theorem 7, we have

$$\begin{aligned}
\frac{da(t)}{dt} &= \frac{d}{dt} \sum_k P(k) a_k(t) = \sum_k P(k) \frac{da_k(t)}{dt} \\
&= \sum_k \left(P(k) \alpha(t) \lambda(t) \exp \left(\int_0^t \alpha(x) \lambda(x) dx \right) \right. \\
&\quad \left. \sum_{k'} k P(k' | k) a_{k'}(0) \right) \\
&= \alpha(t) \lambda(t) \exp \left(\int_0^t \alpha(x) \lambda(x) dx \right) C, \tag{23}
\end{aligned}$$

where $C = \langle k \rangle \sum_k \sum_{k'} P(k, k') a_{k'}(0)$, which is given by the initial state and the underlying network topology of information spreading. Eq. 23 implies that the changing rate of the number of active vertices, or the spreading velocity, is a function of time-varying parameters $\alpha(t)$ and $\lambda(t)$ in the improved model.

C. Explicit Expressions of $\alpha(t)$ and $\lambda(t)$

The previous section studies the impact of time-varying parameters on information spreading in general. In this section, we give explicit mathematical expressions of $\alpha(t)$ and $\lambda(t)$ based on empirical studies.

Previous studies [5, 27, 33, 34] have shown that the popularity tendency of different kinds of information in OSNs follows the long-tailed or power-law pattern. Probability $\alpha(t)$ quantifies the popularity of one particular information in the following way,

$$\alpha(t) \triangleq \Pr\{E_1 \text{ happens at time } t\}$$

where E_1 denotes the event that a user aware of the information becomes active, i.e., the user spreads the information. Note that E_1 happens at time ∞ means that the user becomes indifferent, i.e., the user is aware of the information but does not spread it. Thus $\alpha(t)$ satisfies $0 \leq \alpha(t) \leq 1$ and $\int_0^\infty \alpha(t) dt = 1$, and is a probability distribution. To model realistic popularity tendency, we let $\alpha(t)$ follow the Gamma distribution $\Gamma(p, \eta)$ whose density function satisfying

$$p(x; p, \eta) = \frac{x^{p-1} e^{-x/\eta}}{\eta^p \Gamma(p)}, \tag{24}$$

where $x, p, \eta > 0$ and $\Gamma(p)$ is the Gamma function. We approximate $\alpha(t)$ by the value of its density function at t and have $\alpha(t) = p(t; p, \eta)$.

Several studies [21, 34, 35] have found that in the Web and OSNs, user's online behaviors are of daily cycle and the diurnal pattern has a gentle peak. Assume that immediately after they log in, users in SNSes can get all user generated contents (UGCs) that their neighbors have published and shared. Thus $\lambda(t)$ is determined by the temporal pattern of user's log-in behavior. Similarly, we regard $\lambda(t)$ as

$$\lambda(t) \triangleq \Pr\{E_2 \text{ happens at time } t\},$$

where E_2 denotes the event that a user logs in, or is aware of the information spread by his/her active neighbors. We also assume that user logs in every day and denote C_p as the measure of one day period¹⁰. Hence $\lambda(t)$ satisfies $0 \leq \lambda(t) \leq 1$, $\int_0^{C_p} \lambda(t) dt = 1$ and $\lambda(t) = \lambda(t + C_p)$, and is a periodic distribution. We make $\lambda(t)$ follow a popular circular distribution, the *von Mises* distribution, or the *circular normal* [36], whose density distribution is

$$p(x; z, \vartheta) = \frac{1}{2\pi I_0(z)} \exp(z \cos(x - \vartheta)), \tag{25}$$

where ϑ corresponds to the mean of the distribution, z is known as the *concentration* parameter and

$$I_0(z) = \frac{1}{2\pi} \int_0^{2\pi} \exp(z \cos \vartheta) d\vartheta.$$

Note that the von Mises distribution is of period 2π . To model $\lambda(t)$ with period C_p , we perform variable transformation to Eq. 25 and get

$$\lambda(t) = \frac{1}{C_p I_0(z)} \exp \left(z \cos \left(\frac{2\pi}{C_p} t - \vartheta \right) \right). \tag{26}$$

In general, user's activity pattern represented by $\lambda(t)$ is fixed on average, and the popularity tendency quantified by $\alpha(t)$ varies to different information. Given the constant in Eq. 23, there are six unknown parameters to be determined, i.e., $\Theta = \{p, \eta, z, \vartheta, C_p, C\}$. According to Eq. 23, given the initial conditions, we find that the shape of the time series curve da/dt is controlled by $\alpha(t) \lambda(t) \exp \left(\int_0^t \alpha(x) \lambda(x) dx \right)$. Since this equation is intractable, we adopt the LM algorithm to learn Θ in Section VI.

VI. EXPERIMENTS

In this section, we first present several numerical solutions on the system of Eqs. 1a to 1d based on the model proposed in Section II. These numerical results verify analytic results given in Section IV. Furthermore, for the improved time-varying model, we use LM to learn key parameters derived in Section V, based on a data set of video sharing in Renren. We find that the synthetic curves generated by the time-varying model after learning match the realistic time series precisely. This verifies the accuracy of our model, as well as gives the underlying explanation of the dynamic patterns of information spreading in OSNs. At last, we use Eq. 23 to predict the remaining part of video sharing time series given the initial spreading dynamics. Compared to traditional time series analysis approach, our model works much better and succeeds in predicting future dynamics in the long range.

¹⁰Since the time measure in the model does not correspond to real time, we here set the time period as another parameter.

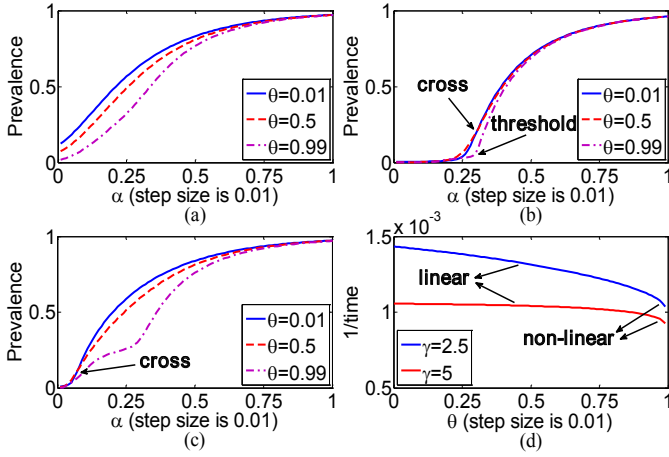


Fig. 4. Spreading dynamics in correlated SF networks. (a) Prevalence \mathcal{P} in the SF network with $\gamma = 2.5$ and $k_c = 473$ is plotted as a function of α . We change α for every 0.01. The results are shown for three values of correlation parameter θ . (b) Prevalence \mathcal{P} in the SF network with $\gamma = 5$ is plotted as a function of α . We find clear turning points and crosses in curves. (c) Prevalence \mathcal{P} in the SF network with $\gamma = 2.5$ but $k_c = 22$ is plotted as a function of α . The crosses in curves come back in the network with small k_c but the same exponent γ as that in (a). (d) Reciprocal of numerical iteration number of system Eqs. 1a to 1d, regarded as the spreading efficiency, is shown for different correlation parameter θ . Two degree distributions of $\gamma = 2.5$ and $\gamma = 5$ are considered. We find approximate negative linear relation between efficiency and degree-degree correlations.

A. Numerical Results of Model with Constant Parameters

In this subsection, we numerically study the dynamics of information spreading in correlated SF networks based on the model with constant parameters. We present numerical solutions using standard finite difference scheme on two SF networks of $\gamma = 2.5$ (heterogeneous) and $\gamma = 5$ (homogeneous) with $k_c = 473$ and $k_c = 11$, respectively. The power-law degree sequences of the exponent-varying networks are generated by the algorithm proposed in [37]. The sizes of these networks are both $n = 10^4$. We set the model parameters as $\lambda = 1$ and $\beta = 0.3$, and increase the value of α from 0.01 to 1 with the step size of 0.01. We investigate how the spreading prevalence \mathcal{P} changes along with the varying α . Note that values of \mathcal{P} are averaged over 100 random equivalent solutions, i.e., we randomly choose one initial active vertex and leave others ignorant each time, and at the same time keep all the model and network parameters unchanged.

In Fig. 4a, the results for the SF network with $\gamma = 2.5$ are shown. As λ and β are fixed, the spreading threshold is only related to α . In this case, we observe the absence of the threshold, which agrees with the conclusion in Remark 4. Whereas in the case of less heterogeneous network with $\gamma = 5$, as shown in Fig. 4b, we observe explicit thresholds of information spreading. Moreover, the threshold in the network with higher positive degree-degree correlations (larger θ) is larger. This verifies the conclusion of Corollary 1 and implies that positive correlations inhibit the spreading process to some extent.

As for the spreading prevalence, Theorem 5 shows that the impact of correlations on prevalence relates to model parameters and the degree distribution. We find that the crosses

of curves plotted in Fig. 4b correspond to the conclusion of Theorem 5, i.e., positive correlations increase the spreading prevalence \mathcal{P} in some values of α while decrease \mathcal{P} in other values. Theorem 5 also holds in the SF network of $\gamma = 2.5$ where k_c is set to be small enough¹¹, e.g., set $k_c = 22$ as that in Fig. 4c. At the same time, in more heterogeneous networks (e.g., $k_c = 473$ in Fig. 4a), the positive correlations inhibit prevalence independent with model parameters. These complicated relations among the spreading prevalence, model parameters and the network topology (e.g., degree distribution, the largest degree and degree-degree correlations) are partly described by Theorem 5. These results also confirm the essential influence of the largest degree on information spreading.

In Fig. 4d, we set model parameters as $\alpha = 0.7$, $\lambda = 1$ and $\beta = 0.3$, and increase the value of θ from 0 to 0.99 with step size of 0.01. We study how correlations influence the spreading efficiency. Note that in Fig. 4d, we take the iteration number of solving system Eqs. 1a to 1d before the spreading process terminates (i.e., there are no active vertices in the network) as the spreading time, whose reciprocal is regarded as the spreading efficiency. The results in Fig. 4d are also averaged over 100 equivalent random solutions. We find approximately negative linear relations when $\theta < 0.9$ between correlations and the efficiency in SF networks of both $\gamma = 2.5$ and $\gamma = 5$. Moreover, with the same θ , information spreads faster in more heterogeneous network (smaller γ and larger $\langle k^2 \rangle / \langle k \rangle$). These numerical results conform to the conclusion in Theorem 6. Note that the non-linear tails of two curves in Fig. 4d result from approximation errors in the proof of Theorem 6 as θ becomes large.

The relations between the spreading process and the underlying network topology (heterogeneity and correlations) are complicated according to both our theoretical analysis in previous sections and numerical studies in this subsection. However, we find that in general, the network heterogeneity improves information spreading in OSNs whereas positive degree-degree correlations inhibit it.

B. Learning Dynamic Patterns of Video Sharing in Renren

From Fig. 2, we have seen that the model with constant parameters cannot characterize dynamic patterns of information spreading in networks subtly. Thus we propose an improved model with time-varying parameters, which can reflex changes in the information popularity and user behavior. This subsection provides detailed experiments on how well the time-varying model characterizes the information spreading process in realistic OSNs.

Our video sharing data set is provided by Renren, one of the most popular SNSes in China. When a user shares a uniform resource locator (URL) of a video from an outside video-sharing site (VSS) to Renren, it becomes a seed and would spread on the network through being re-shared by neighbors of the initial sharing user and neighbors of neighbors of the initial user and so on. This process terminates once no one re-shares

¹¹Although generally speaking, small exponents of SF networks lead to the existence of large degree vertices with high probabilities, they are not negatively related in a deterministic manner.

the URL any more. We find that this is exactly the process described in Section II where our model comes from. Note that all kinds of information (e.g., messages, blogs, photos) in Renren spread in the network in the same manner.

The data set consists of over 7.5 millions logs on video sharing for a week from September 10th to 16th, 2012. Each log records sharing time, user identity numbers and video URLs. And the whole logs contain 335,283 video URLs of which the largest sharing number is 154,955. Note that the number of videos shared in this period should be smaller than the number of URLs, as the same video may share different URLs. Limited by the data set, we consider each URL as a unique video in this subsection.

To preprocess the data set, we first select 1000 top sharing URLs with at least 861 shares. This process is reasonable since popular URLs spread in a larger scale than unpopular ones, and thus they can tell us more about the features of information spreading in OSNs. We then construct time series that record sharing number every thirty minutes based on the selected logs. These time series finally correspond to curves characterized by Eq. 23 and are objects we decide to model. The time-varying model is verified if these two curves fit well. In any case, we prefer somewhat smooth curves than fluctuated ones as we concern more on general shapes of time series curves, which reflect the characteristics of spreading dynamics in essence. However, realistic time series oscillate intensely due to countless uncertainties. To reduce fluctuations and eliminate noises in curve fitting, we apply the Gaussian smoothing on each time series.

Up to now, the experimental verification becomes the problem of curve fitting between preprocessed time series of video sharing and the curves determined by Eq. 23. To test the description ability of Eq. 23, we need to perform curve fitting on different time series. It is a waste of time to carry it out on each time series as many examples share common shapes. This reminds us to first cluster time series and then fit Eq. 23 to the centroid of each cluster. We here adopt the K-Spectral Centroid (K-SC) clustering algorithm¹² proposed by Yang and Leskovec [22], which focuses on pure curve patterns invariant to scaling and translation. In K-SC clustering, the distance $\hat{d}(x, y)$ between time series x and y is defined as [38]

$$\hat{d}(x, y) = \min_{\nu, h} \frac{\|x - \nu y_{(h)}\|}{\|x\|}, \quad (27)$$

where $y_{(h)}$ is the time series after shifting y by h time units and $\|\cdot\|$ is the l_2 norm.

Similar to K-means clustering algorithm, K-SC clustering needs to set the number of clusters manually. To obtain the optimal number of clusters, we measure the quality of clustering in different cluster numbers based on the Average Silhouette [39] and the Hartigan's Index [40]. Note that the distance measures of time series in these indices are computed by Eq. 27. We find from Fig. 5 that the two measures on clustering quality in different cluster numbers do not agree with each other since they measure the clustering quality in

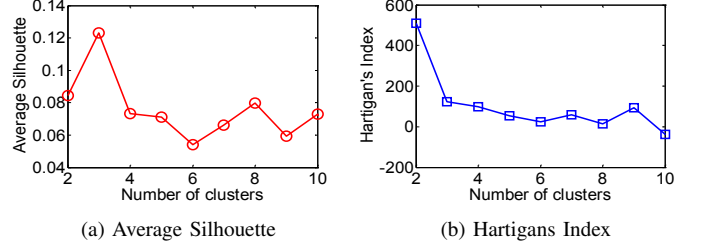


Fig. 5. Clustering quality versus the number of clusters. (a) The average Silhouette measures the tightness of grouped data in the cluster and the separability among clusters in compromise. (b) The Hartigan's Index is a relative measure of the square error decrease as the number of clusters increases.

different perspectives and K-SC cannot satisfy both. Hartigan [40] suggested we should choose the smallest number whose Hartigan's Index is smaller than a number (we set 200 here) as the best cluster number. At the same time, the number with the largest average Silhouette is the ideal cluster number. Hence we conclude that *three* is the most reasonable cluster number. The centroids of clusters C_1 , C_2 and C_3 generated after the algorithm converges are presented in Fig. 6. Note that the centroids are not realistic time series in the data set. They are computed by the K-SC algorithm and represent the general shapes of time series curves in each cluster.

We find from Fig. 6 that three centroids express obvious patterns of time series. Time series in cluster C_1 own one spiky peak and a long tail which contains several gentle peaks. They may come from the videos that gain user's attentions for a moment and then lose their attractions rapidly. As a limitation, the data set cannot record the exact whole process of each video sharing, thus some of the time series in C_1 may also represent the ending process of video sharing. Centroid of C_2 is similar to the curve in Fig. 2b, which is the typical time series of video sharing. Periodic peaks and gradual decay are general characteristics of dynamic patterns of video sharing in Renren. Also limited by the data set, a large number of time series are truncated before terminating, which results in the cluster C_3 . Time series in C_3 could be classified into C_2 in a longer period of time. Therefore, we need to fit Eq. 23 to time series of C_1 and C_2 to test the improved model.

We apply the LM algorithm [23], a standard algorithm to solve non-linear least squares problems, to do curve fitting (i.e., to learn the best parameters in Eq. 23 based on realistic time series). Because centroids are not realistic time series, we first select representative time series s_1 and s_2 of cluster C_1 and C_2 by minimizing the distances defined by Eq. 27, respectively, i.e.,

$$s_1 = \arg \min_{s \in C_1} \hat{d}(s, c_1) \text{ and } s_2 = \arg \min_{s \in C_2} \hat{d}(s, c_2),$$

where c_1 and c_2 are centroids of C_1 and C_2 , respectively. Note that s_1 and s_2 are recovered from Gaussian smoothing for fairness. The results of curve fitting on s_1 and s_2 are presented in Tab. I and Fig. 7.

As there is a great difference in time measures between the model and realistic scenarios, we should first balance two time measures. In fact, the spreading process in the model is much

¹²Although realistic time series exhibit burstiness and periodicity, which induce many noises in clustering, here we just perform clustering on the whole time series roughly to prevent from selecting by hand.

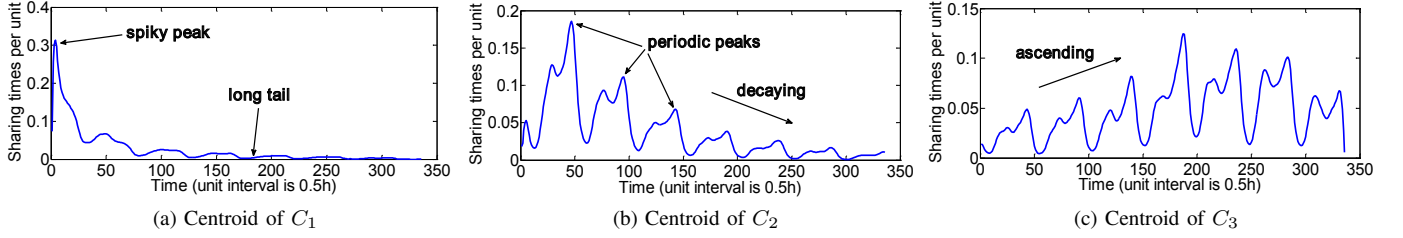
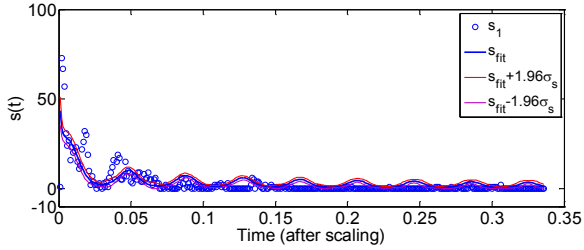


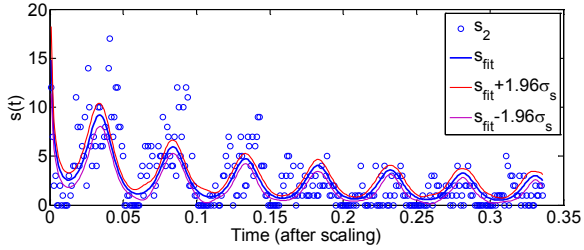
Fig. 6. Cluster centroids generated by the K-SC algorithm. Centroids are not realistic time series in the data set but are generated by K-SC.

TABLE I
PARAMETER VALUES LEARNED BY THE LM ALGORITHM

Θ	p	η	z	ϑ	C_p	C
s_1	0.4677	10.0662	0.8443	1.4631	0.0395	0.1586
s_2	0.5157	11.5924	-0.9050	1.3159	0.0493	0.2382



(a) Curve fitting of time series s_1 in C_1



(b) Curve fitting of time series s_2 in C_2

Fig. 7. Curve fitting on representative time series of C_1 and C_2 . The scale between real time and model time is adjusted to 500:1 (in hour). We also plot the 95% confidence interval (red and purple curves) of the fit, where σ_s is the asymptotic standard parameter error that measures how unexplained variability in the data propagates to variability in the parameters.

faster than that in real world. In our experiments, we set the scale between the real time and model time as 500:1 (in hour), which means that one step in model time equals to 500 hours in real world. We find from Fig. 7 that Eq. 23 derived from the time-varying model fits the time series of video sharing in Renren very well. Specifically, the model can characterize two major features of information spreading in OSNs, i.e., gradual decay and periodic spiky peaks, via two parameters $\alpha(t)$ and $\lambda(t)$ that depict information popularity and user behavior, respectively. Note that limited by somewhat coarseness of the von Mises distribution, Eq. 23 cannot model more delicate features in time series, such as two local maximum always appear in one big peak (see Fig. 6b and Fig. 6c). We believe

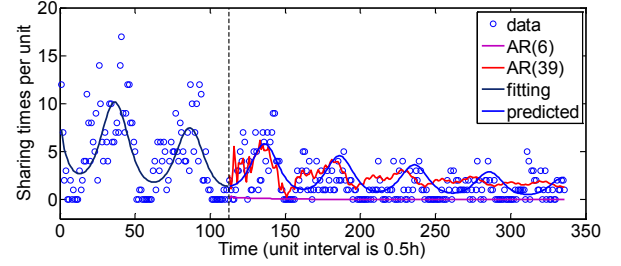


Fig. 8. Comparison of prediction performance of AR and the improved model on time series s_2 . The first 1/3 part (about 56 hours) of s_2 is given to train models. Prediction performances of the remaining 2/3 (about 112 hours) are shown. Note that there are totally 6 parameters in our model. For fairness, we set the order (i.e., the number of regression coefficients) of AR as 6 as well. We also increase the order to 39 for a better prediction performance.

that if $\lambda(t)$ is defined as other periodic distributions¹³ with two or more local maximums, the time-varying model can characterize more detailed features of information spreading in OSNs.

C. Predicting Temporal Dynamics of Video Sharing in Renren

Other than characterizing dynamic patterns of video sharing in Renren, our improved model with time-varying parameters can be used to carry out more realistic task — to predict future temporal dynamics of time series whose head part is given. Here is our idea: given the first part of time series, we learn parameters in Eq. 23 using the LM algorithm the same as what we do in Section VI-B. Then Eq. 23 determines how the time series evolve in the future and we can use this equation to predict the last part of time series. We take the representative time series s_2 as an example. We first truncate the first 1/3 part of s_2 and learn Θ by the LM curve fitting. This gives $p = 0.8822$, $\eta = 0.2461$, $z = -0.7737$, $\vartheta = 1.5292$, $C_p = 0.0498$, $C = 0.0586$. Then we use Eq. 23 equipped with these parameters to generate time series of the remaining 2/3 part. The traditional time series analysis approach, the Autoregressive (AR) model [41], is used to compare with our method. Similarly, we estimate parameters of AR based on the first 1/3 of time series and predict the remaining part with the learned AR. Detailed results are shown in Fig. 8.

From Fig. 8, we find that our model is very good at predicting time series in a long range (see the blue curve in Fig. 8). While AR with the same number of parameters fails to

¹³However, to our knowledge, there are few periodic distributions of this kind.

predict future dynamics and degrades to zero immediately (see the purple curve in Fig. 8). In fact, if we increase the order of AR to 39, more than 6 times of the parameter number of our model, AR can characterize future dynamics as well. But the performance is also not as good as ours. The relative errors [4], which are defined as $\sqrt{\sum_t (s(t) - \tilde{s}(t))^2} / \sqrt{\sum_t s(t)^2}$ where $\tilde{s}(t)$ is the predicted value, are 0.9828, 0.7156, 0.7046 for AR(6), AR(39) and our model, respectively.

VII. RELATED WORK

Representative studies on epidemic spreading [6–13] lay the foundations for studying spreading process in complex networks. Classic epidemic models, such as susceptible-infected-susceptible (SIS) and susceptible-infected-removed (SIR) models, have been studied extensively. Similar to epidemic spreading, rumor diffusion [14–17] can be investigated in the same principle. The main difference between epidemic and rumor spreading is that vertices do not always act actively or react to received messages in rumor diffusion. This leads to related modifications of rumor models [17].

Many other works model the information spreading process in OSNs in different assumptions. Two standard models in innovation diffusion [42], i.e., *Independent Cascades* (IC) and *Linear Threshold* (LT), have been widely employed to model information spreading in OSNs. Galba *et al.* [2] proposed a model based on the LT model to predict information cascades in Twitter¹⁴. Similarly, Guille *et al.* [3] proposed an IC-based model with time-varying parameters to predict temporal dynamics of information spreading in Twitter. Also to predict temporal dynamics of information spreading, Yang *et al.* [4] proposed the so-called Linear Influence Model (LIM) ignorant with the underlying network topology. As LIM mainly focuses on the temporal dynamics of spreading, the influence of vertices is assumed to be the only factor impacting the spreading process. In addition, Leskovec *et al.* [5] used SIS to model blog citing in the blogosphere. All these models either characterize information spreading with finer granularity, or treat the spreading process in different perspectives. However, some of them are too naive to recover realistic temporal dynamics, let alone model dynamic patterns explicitly. Some others do not take network topology into consideration, which indeed highly influences information spreading in OSNs. Even if some do this, they cannot give definite analytic results to show how the network topology influences the spreading process. To understand more related work on information spreading in OSNs, readers can refer to [43].

VIII. CONCLUSION AND FUTURE WORK

In this paper, we first propose a probabilistic spreading model based on IMCs, which features realistic process of information spreading in OSNs. These IMCs also take the underlying network topology (e.g., degree distributions and degree-degree correlations) into account. Then we derive a dynamical system from the original IMCs based on the mean-field principle. With these coupled differential equations

(Eqs. 1a to 1d), we analyze the impact of network topology on information spreading in OSNs. Our theoretical and numerical results show that the network heterogeneity promotes the spreading process, while the positive degree-degree correlations inhibit information spreading in general.

To characterize the temporal dynamics of information spreading in OSNs, we further propose an improved model with time-varying parameters that depict user behavior evolution and information popularity. We derive an explicit function (Eq. 23) to model dynamic patterns of the spreading process. Our experiments show that by learning relevant parameters in the function using the curve fitting algorithm, our improved model can reproduce temporal dynamics of video sharing in Renren precisely. Given historical measurements, the improved model is also able to accurately predict future spreading dynamics in the long range.

Several questions remain to be answered. In the aspect of spreading strategy, we identify vertex influence with each other at present. While in reality the influence of vertices varies a lot and is unnecessarily related to vertex degree [44]. How to differentiate those influential vertices in the probabilistic model needs further study. In network topology, we currently only consider two orders of correlations in the network. Although these correlations have been found in realistic OSNs widely [24], they are not the only factors influencing information spreading. Some other topological features, e.g., the largest degree [8], k -core [44], have been found to impact the spreading process largely. The model needs to be adjusted to express these influences. In model parameters, the spreading rate α is not only related to time but also the influence of vertices as stated above. Moreover, it is recommended [45] to consider indirect links when inspecting ambient influences on one vertex. In this case, α should be calculated by both time and pairwise distances. Note that all the above model improvements should be investigated based on empirical studies.

APPENDIX A

FROM PROBABILISTIC MODEL TO DYNAMICAL SYSTEM

In this section, we derive the dynamical system of Eqs. 1a to 1d from the probabilistic model described in Section II based on the mean-field principle.

Consider a vertex n_j that is ignorant at time t . We denote p_{ii}^j as the probability that n_j stays ignorant in the time interval $[t, t + \Delta t]$. Thus we have $p_{ii}^j = p_{ia}^j + p_{ir}^j = 1 - p_{ii}^j$, where p_{ii}^j , p_{ia}^j , p_{ir}^j are probabilities of n_j changing its state, becoming active, and becoming indifferent, respectively. Let $g = g(t)$ denotes the number of active vertices among n_j 's neighbors at time t , it follows that

$$p_{ii}^j = (1 - \Delta t \lambda)^g.$$

Assume that the degree of n_j is k , and g can be considered as a random variable that has the following binomial distribution,

$$\Pi(g, t) = \binom{k}{g} \psi(k, t)^g (1 - \psi(k, t))^{k-g},$$

¹⁴Twitter. <http://www.twitter.com>.

where $\psi(k, t)$ is the probability at time t that an edge connects an ignorant vertex of degree k with an active vertex. Thus $\psi(k, t)$ can be written as

$$\psi(k, t) = \sum_{k'} P(k' | k) P(a_{k'} | i_k) \approx \sum_{k'} P(k' | k) a_{k'}(t),$$

where we approximate $P(a_{k'} | i_k)$ with $a_{k'}(t)$ by ignoring the correlations between neighboring vertices in different states,

The transition probability $\bar{p}_{ii}(k, t)$ averaged over all possible values of g is given by

$$\begin{aligned} \bar{p}_{ii}(k, t) &= \sum_{g=0}^k \binom{k}{g} (1 - \Delta t \lambda)^g \psi(k, t)^g (1 - \psi(k, t))^{k-g} \\ &= \left(1 - \Delta t \lambda \sum_{k'} P(k' | k) a_{k'}(t) \right)^k. \end{aligned} \quad (\text{A.1})$$

Based on Eq. A.1 we get

$$\bar{p}_{ii}(k, t) = 1 - \bar{p}_{ii}(k, t), \quad (\text{A.2})$$

$$\bar{p}_{ia}(k, t) = \alpha (1 - \bar{p}_{ii}(k, t)), \quad (\text{A.3})$$

$$\bar{p}_{ir}(k, t) = (1 - \alpha) (1 - \bar{p}_{ii}(k, t)). \quad (\text{A.4})$$

From Fig. 1, we have

$$\bar{p}_{aq}(k, t) = \Delta t \beta, \quad (\text{A.5})$$

$$\bar{p}_{aa}(k, t) = 1 - \Delta t \beta. \quad (\text{A.6})$$

Denote $I_k(t)$, $A_k(t)$, $R_k(t)$, $Q_k(t)$ as the expected populations of vertices with degree k that are ignorant, active, indifferent and quiet at time t , respectively. The event that an ignorant vertex with degree k becomes active during $[t, t + \Delta t]$ is a Bernoulli random variable with probability $1 - \bar{p}_{ii}(k, t)$ of success. Since the sum of Bernoulli variables follows the binomial distribution with expectation $I_k(t)(1 - \bar{p}_{ii}(k, t))$, the change of the expected population of ignorant vertices with degree k is

$$\begin{aligned} I_k(t + \Delta t) - I_k(t) &= -I_k(t) \left(1 - \left(1 - \Delta t \lambda \sum_{k'} P(k' | k) a_{k'}(t) \right)^k \right). \end{aligned} \quad (\text{A.7})$$

Similarly, we can get the change of populations of active, indifferent and quiet vertices as follows.

$$\begin{aligned} A_k(t + \Delta t) - A_k(t) &= \alpha I_k(t) \left(1 - \left(1 - \Delta t \lambda \sum_{k'} P(k' | k) a_{k'}(t) \right)^k \right) \\ &\quad - A_k(t) \Delta t \beta. \end{aligned} \quad (\text{A.8})$$

$$\begin{aligned} R_k(t + \Delta t) - R_k(t) &= (1 - \alpha) I_k(t) \left(1 - \left(1 - \Delta t \lambda \sum_{k'} P(k' | k) a_{k'}(t) \right)^k \right). \end{aligned} \quad (\text{A.9})$$

$$Q_k(t + \Delta t) - Q_k(t) = A_k(t) \Delta t \beta. \quad (\text{A.10})$$

For Eqs. A.7 to A.10, we let $\Delta t \rightarrow 0$, omit the higher order infinitesimal and divide each equation by corresponding N_k (the number of vertices with degree k), then finally get Eqs. 1a to 1d.

APPENDIX B PROOF OF THEOREM 1

In uncorrelated heterogeneous networks, the conditional probability $P(k' | k)$ satisfies

$$P(k' | k) = q(k') = \frac{k' P(k')}{\langle k \rangle}.$$

Thus the system of Eqs. 1a to 1d degrades into

$$\frac{di_k(t)}{dt} = -\lambda k i_k(t) \sum_{k'} q(k') a_{k'}(t), \quad (\text{B.1})$$

$$\frac{da_k(t)}{dt} = \alpha \lambda k i_k(t) \sum_{k'} q(k') a_{k'}(t) - \beta a_k(t), \quad (\text{B.2})$$

$$\frac{dr_k(t)}{dt} = (1 - \alpha) \lambda k i_k(t) \sum_{k'} q(k') a_{k'}(t), \quad (\text{B.3})$$

$$\frac{dq_k(t)}{dt} = \beta a_k(t). \quad (\text{B.4})$$

By integrating Eq. B.1, we get

$$i_k(t) = i_k(0) e^{-\lambda k \phi(t)}, \quad (\text{B.5})$$

where $i_k(0) \approx 1$ and

$$\phi(t) = \sum_k q(k) \int_0^t a_k(x) dx = \int_0^t \langle \langle a_k(x) \rangle \rangle dx.$$

Note that we define $\langle \langle \star \rangle \rangle \triangleq \sum_k q(k) \star$.

By multiplying Eq. B.2 with $q(k)$, summing over k and integrating over t , we get

$$\frac{d\phi(t)}{dt} = \langle \langle a_k(t) \rangle \rangle = \alpha - \alpha \langle \langle e^{-\lambda k \phi(t)} \rangle \rangle - \beta \phi(t). \quad (\text{B.6})$$

Let $t \rightarrow \infty$, we have $d\phi/dt \rightarrow 0$, and Eq. B.6 becomes

$$\phi_\infty = \frac{\alpha}{\beta} - \frac{\alpha}{\beta} \sum_k q(k) e^{-\lambda k \phi_\infty}, \quad (\text{B.7})$$

where $\phi_\infty = \lim_{t \rightarrow \infty} \phi(t)$.

It is obvious that $\phi_\infty = 0$ is a trivial solution of Eq. B.7. The non-zero solution exists if only if the condition

$$\left. \frac{d}{d\phi_\infty} \left(\frac{\alpha}{\beta} - \frac{\alpha}{\beta} \sum_k q(k) e^{-\lambda k \phi_\infty} \right) \right|_{\phi_\infty=0} > 1$$

is satisfied, i.e.,

$$\frac{\alpha \lambda}{\beta} > \frac{\langle k \rangle}{\langle k^2 \rangle}. \quad (\text{B.8})$$

Thus we get the threshold $\rho_c = \langle k \rangle / \langle k^2 \rangle$ in uncorrelated heterogeneous networks.

In SF networks, we can calculate $\langle k \rangle$ and $\langle k^2 \rangle$ as follows.

$$\begin{aligned} \langle k \rangle &= \sum_{k=1}^{\infty} k P(k) = Z \sum_{k=1}^{\infty} k^{-\gamma+1} \\ &\approx Z \int_1^{\infty} k^{-\gamma+1} dk = \frac{\gamma-1}{2-\gamma} k^{-\gamma+2} \Big|_1^{\infty}, \end{aligned} \quad (\text{B.9})$$

$$\begin{aligned}\langle k^2 \rangle &= \sum_{k=1}^{\infty} k^2 P(k) = Z \sum_{k=1}^{\infty} k^{-\gamma+2} \\ &\approx Z \int_1^{\infty} k^{-\gamma+2} dk = \frac{\gamma-1}{3-\gamma} k^{-\gamma+3} \Big|_1^{\infty}. \quad (\text{B.10})\end{aligned}$$

To get reasonable result, the networks we consider should have finite average degree. Thus according to Eq. B.9, we have $\gamma > 2$. In addition, $\langle k^2 \rangle < \infty$ if $\gamma > 3$, and $\langle k^2 \rangle = \infty$ otherwise. Hence the spreading threshold of uncorrelated SF networks is given by Eq. 4.

APPENDIX C PROOF OF THEOREM 2

We consider uncorrelated SF networks in this theorem. Denote the spreading prevalence of each degree k as $\mathcal{P}_k = r_k(\infty) + q_k(\infty)$, and we have $\mathcal{P} = \sum_k P(k) \mathcal{P}_k$. Given Eq. B.5, we have

$$\begin{aligned}\mathcal{P} &= \sum_k Z k^{-\gamma} (1 - e^{-\lambda k \phi_{\infty}}) \\ &\approx 1 - (\gamma - 1) \int_1^{\infty} k^{-\gamma} e^{-\lambda k \phi_{\infty}} dk \\ &= 1 - (\gamma - 1) z^{\gamma-1} \int_z^{\infty} x^{-\gamma} e^{-x} dx \\ &= 1 - (\gamma - 1) z^{\gamma-1} \Gamma(-\gamma + 1, z), \quad (\text{C.1})\end{aligned}$$

where $z = \lambda \phi_{\infty}$, $x = \lambda k \phi_{\infty}$ and $\Gamma(s, z)$ is the *incomplete Gamma function*.

As $\Gamma(s, z)$ can be written as

$$\Gamma(s, z) = \Gamma(s) - \int_0^z x^{s-1} e^{-x} dx, \quad (\text{C.2})$$

we perform the Taylor expansion on the integrand of the right-hand side of Eq. C.2 for small z and get

$$\Gamma(s, z) = \Gamma(s) - \frac{z^s}{s} - z^s \sum_{n=1}^{\infty} \frac{(-z)^n}{(s+n)n!}, \quad (\text{C.3})$$

where $\Gamma(s)$ is the *standard Gamma function*. Note that this expansion makes sense only if $s \neq 0, -1, -2, \dots$. The cases of $\gamma \in \mathbb{N}$ should be discussed case by case.

By substituting Eq. C.3 into Eq. C.1, we get

$$\begin{aligned}\mathcal{P} &= \Gamma(-\gamma + 2) z^{\gamma-1} + (\gamma - 1) \sum_{n=1}^{\infty} \frac{(-z)^n}{(n - \gamma + 1)n!} \\ &\approx \frac{\gamma - 1}{\gamma - 2} z + \mathcal{O}(z^{\gamma-1}).\end{aligned}$$

Thus for any $\gamma > 2$, we have

$$\mathcal{P} \approx \frac{\gamma - 1}{\gamma - 2} z = \frac{\gamma - 1}{\gamma - 2} \lambda \phi_{\infty}. \quad (\text{C.4})$$

We will get the expression of \mathcal{P} once ϕ_{∞} is obtained. For Eq. B.7, we perform the same calculations as Eq. C.1 and get

$$\phi_{\infty} = \frac{\alpha}{\beta} - \frac{\alpha}{\beta} (\gamma - 2) z^{\gamma-2} \Gamma(-\gamma + 2, z),$$

which gives

$$\phi_{\infty} = \frac{\alpha}{\beta} z^{\gamma-2} \Gamma(3 - \gamma) + \frac{\alpha}{\beta} (\gamma - 2) \sum_{n=1}^{\infty} \frac{(-z)^n}{(n + 2 - \gamma)n!}. \quad (\text{C.5})$$

The leading behavior of ϕ_{∞} depends on particular values of γ . We consider the following cases.

(1) $2 < \gamma < 3$:

In this case, we have

$$\phi_{\infty} \approx \frac{\alpha}{\beta} (\lambda \phi_{\infty})^{\gamma-2} \Gamma(3 - \gamma),$$

which gives

$$\phi_{\infty} \approx (\Gamma(3 - \gamma))^{1/(3-\gamma)} (\alpha/\beta)^{1/(3-\gamma)} \lambda^{(\gamma-2)/(3-\gamma)}. \quad (\text{C.6})$$

Combining Eq. C.6 with Eq. C.4, we get Eq. 5.

(2) $3 < \gamma < 4$:

According to Eq. C.5, we have

$$\phi_{\infty} \approx \frac{\alpha}{\beta} (\lambda \phi_{\infty})^{\gamma-2} \Gamma(3 - \gamma) - \frac{\alpha}{\beta} \frac{\gamma - 2}{3 - \gamma} \lambda \phi_{\infty},$$

which gives

$$\phi_{\infty} \approx \left(\frac{\beta}{\alpha \lambda^{\gamma-2}} \frac{\gamma - 2}{\Gamma(4 - \gamma)} \left(\frac{\alpha \lambda}{\beta} - \frac{\gamma - 3}{\gamma - 2} \right) \right)^{1/(\gamma-3)}. \quad (\text{C.7})$$

Combining Eq. C.7 with Eq. C.4, we get Eq. 6.

(3) $\gamma > 4$:

The dominant terms in the expansion of ϕ_{∞} are now

$$\phi_{\infty} \approx \frac{\alpha}{\beta} \frac{\gamma - 2}{\gamma - 3} \lambda \phi_{\infty} - \frac{\alpha}{2\beta} \frac{\gamma - 2}{\gamma - 4} (\lambda \phi_{\infty})^2,$$

which gives

$$\phi_{\infty} \approx \frac{2(\gamma - 4)}{\gamma - 3} \frac{\beta}{\alpha \lambda^2} \left(\frac{\alpha \lambda}{\beta} - \frac{\gamma - 3}{\gamma - 2} \right). \quad (\text{C.8})$$

Combining Eq. C.8 with Eq. C.4, we get Eq. 7.

(4) $\gamma = 3$:

By carrying out similar approximation techniques as those in cases (1) to (3) except making use of the expansion of $\Gamma(0, z)$ as $z \rightarrow 0$, i.e.,

$$\Gamma(0, z) = -(\gamma_E + \ln(z)) + z + \mathcal{O}(z^2), \quad (\text{C.9})$$

where γ_E is the Euler's constant, instead of the expansion Eq. C.3, we can get Eq. 8. For brevity, we omit the detailed proof here.

APPENDIX D PROOF OF THEOREM 3

By omitting terms of $\mathcal{O}(a^2)$, we can write Eq. B.2 as

$$\begin{aligned}\frac{da_k(t)}{dt} &\approx \alpha \lambda k \sum_{k'} q(k') a_{k'}(t) - \beta a_k(t) \\ &= \alpha \lambda k \langle \langle a_k(t) \rangle \rangle - \beta a_k(t), \quad (\text{D.1})\end{aligned}$$

where $\langle \langle a_k(t) \rangle \rangle$ is a function of t with $\langle \langle a_k(0) \rangle \rangle \approx a(0) \approx 1$. Then the change rate equation of $\langle \langle a_k(t) \rangle \rangle$ can be written as

$$\begin{aligned}\frac{d\langle \langle a_k(t) \rangle \rangle}{dt} &= \sum_k q(k) \frac{da_k(t)}{dt} \\ &= \sum_k q(k) (\alpha \lambda k \langle \langle a_k(t) \rangle \rangle - \beta a_k(t)) \\ &= \alpha \lambda \left(\frac{\langle k^2 \rangle}{\langle k \rangle} - \frac{\beta}{\alpha \lambda} \right) \langle \langle a_k(t) \rangle \rangle. \quad (\text{D.2})\end{aligned}$$

By solving Eqs. D.2 and D.1, we have

$$\langle \langle a_k(t) \rangle \rangle = e^{t/\tau} \quad (\text{D.3})$$

and

$$a_k(t) = e^{-\beta t} \left(1 + \frac{k \langle k \rangle}{\langle k^2 \rangle} \left(e^{(\frac{1}{\tau} + \beta)t} - 1 \right) \right), \quad (\text{D.4})$$

where τ is given by Eq. 9.

For the total number of active vertices $a(t)$ which equals to $\sum_k P(k) a_k(t)$, we have

$$a(t) = e^{-\beta t} \left(1 + \frac{\langle k \rangle^2}{\langle k^2 \rangle} \left(e^{(\frac{1}{\tau} + \beta)t} - 1 \right) \right). \quad (\text{D.5})$$

Note that $e^{t/\tau}$ is the dominant term of Eqs. D.4 and D.5. Furthermore, for uncorrelated SF networks, Eq. 10 can be get easily from Eq. 9 given Eqs. B.9 and B.10. This completes the proof.

APPENDIX E PROOF OF THEOREM 4

We consider correlated heterogeneous networks (i.e., Markovian networks) in this theorem. Consider the Jacobian matrix \mathbf{L} defined as Eq. 13, the solution $\mathbf{a} = \mathbf{0}$ is unstable if there exists at least one positive eigenvalue of \mathbf{L} .

Based on Eq. 3, we have the connectivity detailed balance condition [6]

$$kP(k'|k)P(k) = k'P(k|k')P(k') = \langle k \rangle P(k, k'). \quad (\text{E.1})$$

As to the connectivity matrix \mathbf{C} , if (v_k) is an eigenvector of \mathbf{C} with eigenvalue Λ , then by Eq. E.1, $(P(k)v_k)$ is an eigenvector of \mathbf{C}^\top with the same eigenvalue. Hence all eigenvalues of \mathbf{C} are real. Let Λ_m be the largest eigenvalue of \mathbf{C} . Since $\mathbf{L} = \alpha\lambda\mathbf{C} - \beta\mathbf{I}$, the largest eigenvalue of \mathbf{L} is $\alpha\lambda\Lambda_m - \beta$. Therefore, \mathbf{L} has at least one positive eigenvalue whenever $\alpha\lambda\Lambda_m - \beta > 0$. This gives the threshold $\rho_c = 1/\Lambda_m$.

APPENDIX F PROOF OF THEOREM 5

The proof techniques used here are similar to those in the proof of Theorem 2.

By integrating Eq. 17a, we get

$$i_k(t) = i_k(0)e^{-\lambda k \phi_k(t)}, \quad (\text{F.1})$$

where

$$\phi_k(t) = (1 - \theta)\phi(t) + \theta \int_0^t a_k(x) dx \quad (\text{F.2})$$

and $\phi(t)$ is defined in Appendix B. Given $a_k(0) \approx 0$, we integrate Eq. 17b and have

$$a_k(t) = \alpha - \alpha i_k(t) - \beta \int_0^t a_k(x) dx.$$

Since $a_k(\infty) = a_\infty = 0$, we have

$$\int_0^\infty a_k(x) dx = \frac{\alpha}{\beta} (1 - i_k(\infty)). \quad (\text{F.3})$$

By combining Eqs. F.1, F.2 and F.3, we have

$$\begin{aligned} \phi_k(\infty) &= (1 - \theta)\phi_\infty + \theta \int_0^\infty a_k(x) dx \\ &= (1 - \theta)\phi_\infty + \frac{\alpha\theta}{\beta} (1 - e^{-\lambda k \phi_k(\infty)}). \end{aligned} \quad (\text{F.4})$$

By performing the Taylor expansion on $e^{-\lambda k \phi_k(\infty)}$ of Eq. F.4 and omitting higher-order terms, we get

$$\phi_k(\infty) = \frac{1 - \theta}{1 - \theta\rho k} \phi_\infty. \quad (\text{F.5})$$

Given Eqs. F.1 and F.5, we have

$$\begin{aligned} \mathcal{P} &= \sum_k P(k) \mathcal{P}_k = \sum_k Z k^{-\gamma} (1 - e^{-\lambda k \phi_k(\infty)}) \\ &= 1 - (\gamma - 1) \int_1^\infty k^{-\gamma} e^{-\frac{(1-\theta)\lambda k}{1-\theta\rho k} \phi_\infty} dk, \end{aligned} \quad (\text{F.6})$$

where $1/(1 - \theta\rho k)$ can be expanded as

$$\frac{1}{1 - \theta\rho k} = \sum_{n=0}^\infty (\theta\rho k)^n$$

when $\theta\rho k < 1$. At the same time, part of the integrand in Eq. F.6, $\exp\left(-\frac{(1-\theta)\lambda k}{1-\theta\rho k} \phi_\infty\right)$, can be written as

$$e^{-\frac{(1-\theta)\lambda k}{1-\theta\rho k} \phi_\infty} = e^{\left(\frac{(1-\theta)\lambda}{\theta\rho} \phi_\infty\right) / \left(1 - \frac{1}{\theta\rho k}\right)},$$

where $1 / \left(1 - \frac{1}{\theta\rho k}\right)$ has the expansion

$$1 / \left(1 - \frac{1}{\theta\rho k}\right) = \sum_{n=0}^\infty \left(\frac{1}{\theta\rho k}\right)^n$$

when $\theta\rho k > 1$.

Now we analyze relations between \mathcal{P} and θ on a case-by-case basis.

(1) $\gamma > 2$ and $\gamma \notin \mathbb{N}$:

In this case, we have the following Eq. F.7, where $x_1 = (1 - \theta)\lambda\phi_\infty$, $x_2 = x_1/\theta\rho$, $A_1 = ((\theta\rho)^{\gamma-2} - 1)^{\frac{\gamma-1}{\gamma-2}}$, $A_2 = -(\theta\rho)^{\gamma-1}$, and $\theta\rho k_1 = 1$. Note that if $k < \lfloor k_1 \rfloor$, then $\theta\rho k < 1$, and if $k > \lceil k_1 \rceil$, then $\theta\rho k > 1$.

Moreover, we write Eq. F.7 as

$$\mathcal{P} = (A_1 + A_2 x^{-1}) (1 - \theta)\lambda\phi_\infty, \quad (\text{F.8})$$

where $x = \theta\rho$. Note that in the calculation of Eq. F.8 and the following Eq. F.9, we use the Taylor expansion of $\Gamma(s, z)$, i.e., Eq. C.3. Thus Eqs. F.8 and F.9 make sense only if $\gamma \notin \mathbb{N}$. The cases of $\gamma \in \mathbb{N}$ should be discussed case by case.

By multiplying Eq. 17b with $q(k)$, summing over k and integrating over t , we get

$$\frac{d\phi(t)}{dt} = \alpha - \alpha \langle \langle e^{-\lambda k \phi_k(t)} \rangle \rangle - \beta \phi(t).$$

As $t \rightarrow \infty$, we have $d\phi/dt \rightarrow 0$. Then we get

$$\phi_\infty \approx \frac{\alpha}{\beta} \left(1 - (\gamma - 2) \int_1^\infty k^{-\gamma+1} e^{-\lambda k \phi_k(\infty)} dk \right),$$

which is similar to Eq. F.6. Hence we use the same technique and obtain

$$\phi_\infty \approx \frac{\alpha}{\beta} (B_1 x_1 + B_2 x_1^2 + B_3 x_2)$$

$$\begin{aligned}
\mathcal{P} &= 1 - (\gamma - 1) \left(\int_1^{\lfloor k_1 \rfloor} k^{-\gamma} e^{-(1-\theta)\lambda k \phi_\infty} \sum_{n=0}^{\infty} (\theta \rho k)^n dk + \int_{\lfloor k_1 \rfloor}^{\infty} k^{-\gamma} e^{\frac{(1-\theta)\lambda}{\theta \rho} \phi_\infty} \sum_{n=0}^{\infty} \left(\frac{1}{\theta \rho k}\right)^n dk \right) \\
&\approx 1 - (\gamma - 1) \left(\int_1^{\lfloor k_1 \rfloor} k^{-\gamma} e^{-(1-\theta)\lambda k \phi_\infty} dk + \int_{\lfloor k_1 \rfloor}^{\infty} k^{-\gamma} e^{\frac{(1-\theta)\lambda}{\theta \rho} \phi_\infty} dk \right) \\
&= 1 - (\gamma - 1) \left(x_1^{\gamma-1} (\Gamma(-\gamma + 1, x_1) - \Gamma(-\gamma + 1, x_1 \lfloor k_1 \rfloor)) + \frac{\lfloor k_1 \rfloor^{-\gamma+1}}{\gamma - 1} e^{x_2} \right) \\
&\approx A_1 x_1 + A_2 x_2.
\end{aligned} \tag{F.7}$$

$$= (B_1 + B_2(1 - \theta)\lambda \phi_\infty + B_3 x^{-1}) (1 - \theta)\rho \phi_\infty,$$

where x_1, x_2 and x have the same meaning as those in Eq. F.7, and $B_1 = ((\theta \rho)^{\gamma-3} - 1) \frac{\gamma-2}{\gamma-3}$, $B_2 = ((\theta \rho)^{\gamma-4} - 1) \frac{\gamma-2}{2(\gamma-4)}$, $B_3 = -(\theta \rho)^{\gamma-2}$. Then we have

$$(1 - \theta)\lambda \phi_\infty = \frac{1 - (1 - \theta)\rho B_1 - (1 - \theta)\rho B_3 x^{-1}}{(1 - \theta)\rho B_2}. \tag{F.9}$$

Given Eqs. F.8 and F.9, we get

$$\mathcal{P} = \frac{p_1(\theta)}{p_2(\theta)}, \tag{F.10}$$

where γ is fixed, $p_1(\theta)$ and $p_2(\theta)$ are polynomials of θ , and their coefficients are polynomials of ρ . This implies that, given γ , the impact of θ on \mathcal{P} is related to ρ , i.e., there exists a real number $c_0(\gamma)$ such that the degree-degree correlations promote the spreading prevalence if $\rho < c_0(\gamma)$, whereas inhibit the prevalence if $\rho > c_0(\gamma)$. Note that the opposite case is also possible.

(2) $\gamma = 3$:

The approximation techniques used here are similar to those in case (1) except making use of Eq. C.9 instead of Eq. C.3. The conclusion of this case is the same as that of case (1). For brevity, we omit the detailed proof here.

REFERENCES

- [1] T. Sakaki, M. Okazaki, and Y. Matsuo, "Earthquake shakes Twitter users: real-time event detection by social sensors," in *Proc. WWW*, 2010.
- [2] W. Galuba, K. Aberer, D. Chakraborty, Z. Despotovic, and W. Kellerer, "Outtweeting the twitterers – predicting information cascades in microblogs," in *Proc. WOSN*, 2010.
- [3] A. Guille and H. Hacid, "A predictive model for the temporal dynamics of information diffusion in online social networks," in *Proc. WWW*, 2012.
- [4] J. Yang and J. Leskovec, "Modeling information diffusion in implicit networks," in *Proc. IEEE ICDM*, 2010.
- [5] J. Leskovec, M. McGlohon, C. Faloutsos, N. Glance, and M. Hurst, "Patterns of cascading behavior in large blog graphs," in *Proc. SIAM SDM*, 2007.
- [6] M. Boguñá and R. Pastor-Satorras, "Epidemic spreading in correlated complex networks," *Phys. Rev. E*, vol. 66, p. 047104, 2002.
- [7] Y. Moreno, R. Pastor-Satorras, and A. Vespignani, "Epidemic outbreaks in complex heterogeneous networks," *Eur. Phys. J. B*, vol. 26, pp. 521–529, 2002.
- [8] R. Pastor-Satorras and A. Vespignani, "Epidemic dynamics in finite size scale-free networks," *Phys. Rev. E*, vol. 65, p. 035108, 2002.
- [9] M. Boguñá, R. Pastor-Satorras, and A. Vespignani, "Absence of epidemic threshold in scale-free networks with degree correlations," *Phys. Rev. Lett.*, vol. 90, p. 028701, 2003.
- [10] —, "Epidemic spreading in complex networks with degree correlations," in *Statistical Mechanics of Complex Networks*. Springer Berlin Heidelberg, 2003.
- [11] Y. Moreno, J. B. Gómez, and A. F. Pacheco, "Epidemic incidence in correlated complex networks," *Phys. Rev. E*, vol. 68, p. 035103, 2003.
- [12] M. Barthélemy, A. Barrat, R. Pastor-Satorras, and A. Vespignani, "Velocity and hierarchical spread of epidemic outbreaks in scale-free networks," *Phys. Rev. Lett.*, vol. 92, p. 178701, 2004.
- [13] —, "Dynamical patterns of epidemic outbreaks in complex heterogeneous networks," *J. Theor. Biol.*, vol. 235, pp. 275 – 288, 2005.
- [14] D. J. Daley and D. G. Kendall, "Stochastic rumours," *J. Inst. Math. Appl.*, vol. 1, pp. 42–55, 1965.
- [15] Y. Moreno, M. Nekovee, and A. F. Pacheco, "Dynamics of rumor spreading in complex networks," *Phys. Rev. E*, vol. 69, p. 066130, 2004.
- [16] M. Nekovee, Y. Moreno, G. Bianconi, and M. Marsili, "Theory of rumour spreading in complex social networks," *Physica A*, vol. 374, pp. 457 – 470, 2007.
- [17] J. Borge-Holthoefer, S. Meloni, B. Gonçalves, and Y. Moreno, "Emergence of influential spreaders in modified rumor models," *J. Stat. Phys.*, vol. 151, pp. 383–393, 2013.
- [18] J. Conlisk, "Interactive Markov chains," *J. Math. Sociol.*, vol. 4, pp. 157–185, 1976.
- [19] J. Kleinberg, "Bursty and hierarchical structure in streams," in *Proc. ACM KDD*, 2002.
- [20] M. Vlachos, C. Meek, Z. Vagena, and D. Gunopulos, "Identifying similarities, periodicities and bursts for online search queries," in *Proc. ACM SIGMOD*, 2004.
- [21] F. Benevenuto, T. Rodrigues, M. Cha, and V. Almeida, "Characterizing user behavior in online social networks," in *Proc. ACM IMC*, 2009.
- [22] J. Yang and J. Leskovec, "Patterns of temporal variation in online media," in *Proc. ACM WSDM*, 2011.
- [23] K. Levenberg, "A method for the solution of certain non-linear problems in least squares," *Quart. Appl. Math.*, vol. 2, pp. 164–168, 1944.
- [24] M. Newman, *Networks: An Introduction*. Oxford University Press, Inc., 2010.
- [25] A.-L. Barabási and R. Albert, "Emergence of scaling in random networks," *Science*, vol. 286, pp. 509–512, 1999.
- [26] A. Mislove, M. Marcon, K. P. Gummadi, P. Druschel, and B. Bhattacharjee, "Measurement and analysis of online social networks," in *Proc. ACM IMC*, 2007.
- [27] H. Chun, H. Kwak, Y.-H. Eom, Y.-Y. Ahn, S. Moon, and H. Jeong, "Comparison of online social relations in volume vs interaction: a case study of Cyworld," in *Proc. ACM IMC*, 2008.
- [28] J. Jiang, C. Wilson, X. Wang, P. Huang, W. Sha, Y. Dai, and B. Y. Zhao, "Understanding latent interactions in online social networks," in *Proc. ACM IMC*, 2010.
- [29] M. E. J. Newman, "Assortative mixing in networks," *Phys. Rev. Lett.*, vol. 89, p. 208701, 2002.
- [30] R. Pastor-Satorras, A. Vázquez, and A. Vespignani, "Dynamical and correlation properties of the Internet," *Phys. Rev. Lett.*, vol. 87, p. 258701, 2001.
- [31] S. Garg, T. Gupta, N. Carlsson, and A. Mahanti, "Evolution of an online social aggregation network: an empirical study," in *Proc. ACM IMC*, 2009.
- [32] A. Vázquez and M. Weigt, "Computational complexity arising from degree correlations in networks," *Phys. Rev. E*, vol. 67, p. 027101, 2003.
- [33] A.-L. Barabási, "The origin of bursts and heavy tails in human dynamics," *Nature*, vol. 435, pp. 207–211, 2005.
- [34] M. Cha, H. Kwak, P. Rodriguez, Y.-Y. Ahn, and S. Moon, "Analyzing the video popularity characteristics of large-scale user generated content systems," *IEEE/ACM Trans. Netw.*, vol. 17, pp. 1357–1370, 2009.
- [35] B. Gonçalves and J. J. Ramasco, "Human dynamics revealed through Web analytics," *Phys. Rev. E*, vol. 78, p. 026123, 2008.

- [36] C. M. Bishop, *Pattern Recognition and Machine Learning*. Springer-Verlag New York, Inc., 2006.
- [37] F. Viger and M. Latapy, “Efficient and simple generation of random simple connected graphs with prescribed degree sequence,” in *Proc. COCOON*, 2005.
- [38] K. K. W. Chu and M. H. Wong, “Fast time-series searching with scaling and shifting,” in *Proc. ACM SIGMOD/PODS*, 1999.
- [39] P. J. Rousseeuw, “Silhouettes: A graphical aid to the interpretation and validation of cluster analysis,” *J. Comput. Appl. Math.*, vol. 20, pp. 53 – 65, 1987.
- [40] J. Hartigan, *Clustering algorithms*. John Wiley & Sons, Inc., 1975.
- [41] G. E. P. Box and G. Jenkins, *Time Series Analysis, Forecasting and Control*. Holden-Day, Inc., 1990.
- [42] E. M. Rogers and E. Rogers, *Diffusion of Innovations*. Simon & Schuster, Inc., 2003.
- [43] A. Guille, H. Hacid, C. Favre, and D. A. Zighed, “Information diffusion in online social networks: A survey,” *SIGMOD Rec.*, vol. 42, pp. 17–28, 2013.
- [44] M. Kitsak, L. K. Gallos, S. Havlin, F. Liljeros, L. Muchnik, H. E. Stanley, and H. A. Makse, “Identification of influential spreaders in complex networks,” *Nat Phys*, vol. 6, pp. 888–893, 2010.
- [45] M. B. Ná, C. Castellano, and R. P. Satorras, “Nature of the epidemic threshold for the susceptible-infected-susceptible dynamics in networks,” *Phys. Rev. Lett.*, vol. 111, pp. 068 701+, 2013.